

4-2018

## Modelling the Micro environment of Liver Cancer Using 3D Culture System

Ala'a Abdel Rahim H Al Hrouf

Follow this and additional works at: [https://scholarworks.uaeu.ac.ae/bio\\_theses](https://scholarworks.uaeu.ac.ae/bio_theses)



Part of the [Biology Commons](#), and the [Biotechnology Commons](#)

---

### Recommended Citation

Al Hrouf, Ala'a Abdel Rahim H, "Modelling the Micro environment of Liver Cancer Using 3D Culture System" (2018). *Biology Theses*. 12.

[https://scholarworks.uaeu.ac.ae/bio\\_theses/12](https://scholarworks.uaeu.ac.ae/bio_theses/12)

This Thesis is brought to you for free and open access by the Biology at Scholarworks@UAEU. It has been accepted for inclusion in Biology Theses by an authorized administrator of Scholarworks@UAEU. For more information, please contact [fadl.musa@uaeu.ac.ae](mailto:fadl.musa@uaeu.ac.ae).

**UAEU**



جامعة الإمارات العربية المتحدة  
United Arab Emirates University

United Arab Emirates University

College of Science

Department of Biology

MODELLING THE MICROENVIRONMENT OF LIVER CANCER  
USING 3D CULTURE SYSTEM

Ala'a Abdel Rahim H. Al Hrouf

This thesis is submitted in partial fulfilment of the requirements for the degree of  
Master of Science in Molecular Biology and Biotechnology

Under the Supervision of Professor Amr Amin

April 2018

## Declaration of Original Work

I, Ala'a Abdel Rahim H. Al Hrouf, the undersigned, a graduate student at the United Arab Emirates University (UAEU), and the author of this thesis entitled "*Modelling the Microenvironment of Liver Cancer using 3D culture system*", hereby, solemnly declare that this thesis is my own original research work that has been done and prepared by me under the supervision of Professor Amr Amin, in the College of Science at UAEU. This work has not previously been presented or published, or formed the basis for the award of any academic degree, diploma or a similar title at this or any other university. Any materials borrowed from other sources (whether published or unpublished) and relied upon or included in my thesis have been properly cited and acknowledged in accordance with appropriate academic conventions. I further declare that there is no potential conflict of interest with respect to the research, data collection, authorship, presentation and/or publication of this thesis.

Student's Signature: Ala'a

Date: 8/10/18

## Approval of the Master Thesis

This Master Thesis is approved by the following Examining Committee Members:

- 1) Advisor (Committee Chair): Amr Amin

Title: Professor

Department of Biology

College of Science

Signature



Date

4/23/18

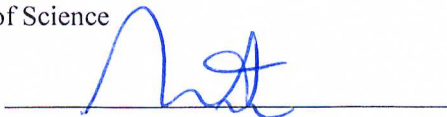
- 2) Member: Synan Abu-Qamar

Title: Associate Professor

Department of Biology

College of Science

Signature



Date

23/4/2018

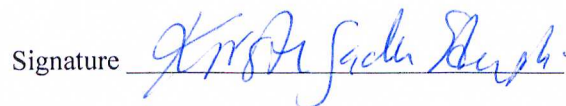
- 3) Member (External Examiner): Kirsten Sadler Edepli

Title: Associate Professor

Division of Science and Math

Institution: New York University Abu Dhabi

Signature

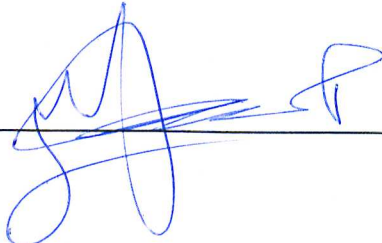


Date

23/4/2018


This Master Thesis is accepted by:

Dean of the College of Science: Professor Ahmed Murad

Signature 

Date 11/10/2018

*for* Dean of the College of Graduate Studies: Professor Nagi T. Wakim

Signature Ali Hassan 

Date 14/10/2018

Copy 3 of 6

Copyright © 2018 Ala'a Abdel Rahim H. Al Hrouf  
All Rights Reserved

## Abstract

Tumor microenvironment has been the focus of many studies that highlighted its essential contribution to tumorigenesis. A two-way communication between the tumor and the surrounding microenvironment sustains and contributes to the growth and metastasis of the tumor by several means, such as extracellular matrix remodeling, fibroblasts activation, epithelial-mesenchymal transition. Hepatocellular carcinoma progression and metastasis have been reported to be highly influenced by diverse microenvironmental elements. The main objective of this study is to create an *in vitro* model of liver cancer microenvironment that better recapitulate *in vivo* settings. The proposed model is based on three-dimensional co-culture system of liver cancer cells and non-malignant fibroblasts. The model presented herein exhibited a transcriptome profile associated with an aggressive phenotype that better mimics *in vivo* hepatocellular carcinoma, and therefore, a more reliable platform for anti-cancer drug screening.

**Keywords:** 3D culture, drug resistance, liver cancer, hepatocellular carcinoma, tumor microenvironment, transcriptome.

## Title and Abstract (in Arabic)

### نمذجة البيئة الميكروية لسرطان الكبد عبر نظام زراعة الخلايا ثلاثي الأبعاد

#### الملخص

البيئة الميكروية للسرطان كانت و ما تزال محط اهتمام دراسات عديدة سلطت الضوء على إسهامها في تكون الأورام. التواصل ثنائي الإتجاه بين الورم السرطاني و البيئة المحيطة به يشارك و يديم النمو و الإنبثاث السرطاني عبر إعادة تصميم النسيج خارج الخلية، تنشيط الخلايا الليفية، و عملية التحول الظهارية المتوسطة. تشير الأبحاث أن البيئة الميكروية تؤثر بقوة على تقدم و إنبثاث سرطان الكبد. الهدف الرئيسي لهذه الأطروحة هو إبتكار نموذج للبيئة الميكروية لسرطان الكبد له القدرة على تمثيل الوسط الحيوي بشكل أفضل. يعتمد النموذج المقترح على نظام زراعة الخلايا ثلاثي الأبعاد لخلايا الكبد السرطانية مع خلايا ليفية غير خبيثة. أبدى ترانسكريبتيوم النموذج تعبير جيني يشير إلى سمات أكثر عدوانية تحاكي سرطان الكبد في الوسط الحيوي، و بالتالي يمثل النموذج منصة فعالة لاختبار العلاجات المضادة للسرطان.

**مفاهيم البحث الرئيسية:** زراعة الخلايا ثلاثية الأبعاد، مقاومة الأدوية، سرطان الكبد، البيئة الميكروية الترانسكريبتوم.



## Acknowledgements

I want to acknowledge and thank all who helped me bring this thesis to completion, by lending an ear or that Bioanalyzer kit I needed.

I would like to express my gratitude to my advisor, Prof. Amr Amin for his continuous support, from the time I joined his lab as an undergraduate, until this moment, where I'm completing my master's thesis. I will always be grateful for his encouragement, pushing me to bring nothing less than my best and allowing me to explore my scientific ideas freely. I would also like to thank my co-advisor, Dr. Kourosch Salehi-Ashtiani for his assistance throughout my research work; giving me access to his lab facilities and workshops needed to complete my thesis; his help made completing this thesis that much easier. Many thanks to Ms. Mehar Sultana and Dr. Amphun Chaiboonchoe at Dr. Kourosch's lab for being more than helpful during my research, assisting me and answering all of my questions and concerns. I would also like to extend my gratitude to Dr. Ali Al Naqbi for his contributions to this thesis; and Zayed Cener for Health Sciences for funding this study.

Special thanks to Dr. Synan Abu-Qamar, for his unrivaled support and guidance throughout my graduate school journey. I would also like to thank him for accepting to be on my examining committee, and extending his help whenever needed. I want to also thank Dr. Kirsten Edepli for accepting to be my external examiner and providing her valuable feedback on my thesis.

Many thanks to Ms. Raja Al-Muskari, Ms. Salwa Sultan, Dr. Mohammed Al Deeb, Dr. Fatima Al-Ansari, Dr. Gaber Ramadan, Dr. David Thomson, and Dr. Mohammed Ayoub at the biology department for their much-needed pep talks. I'm also very grateful to Prof. Thies Thiemann at the chemistry department for his

unbelievable support, encouragement, and guidance inside and outside the classroom. I would also like to thank Ms. Ifrah, Ms. Dhanya, Ms. Nasra, Noor Shehada, and my bench buddies, Badriya, Chandra, and Ameera for their moral (and mental) support throughout my journey at UAEU. I want to express my gratitude to Heba Al Ashram for her great friendship since our time as undergraduates, through the rough patches and tough times, and for her continuous support, encouragement, and boosting my ego overall.

Last, but not least, I would like to express my deepest gratitude to my mother for setting an example of how to carry oneself with undeniable strength and a great deal of grace; for her endless love and support, and for the wonder-filled life she has given me. I would also like to acknowledge my younger siblings, Tariq, Rawan, and Haya, without whom I would have finished my thesis long time ago.

## Dedication

*To my beloved mother, Intisar  
and  
The loving memory of Mustafa Cherkawi*

## Table of Contents

Title .....	i
Declaration of Original Work .....	ii
Copyright .....	iii
Advisory Committee .....	iv
Approval of the Master Thesis .....	vi
Abstract .....	vii
Title and Abstract (in Arabic) .....	viii
Acknowledgements .....	ix
Dedication .....	xii
Table of Contents .....	xiii
List of Tables.....	xiv
List of Figures .....	xv
List of Abbreviations.....	xvi
Chapter 1: Introduction .....	1
1.1 The Tumor Microenvironment .....	1
1.2 Cancer Associated Fibroblasts.....	2
1.3 Hypoxia .....	3
1.4 Hepatocellular Carcinoma .....	5
1.5 Three-dimensional Culture .....	7
1.6 Hypotheses to be tested .....	8
Chapter 2: Materials and Methods .....	10
2.1 Cell Lines.....	10
2.2 2D Culture .....	10
2.3 3D Culture .....	10
2.4 Morphology Assessment .....	11
2.5 Co-culture Systems.....	12
2.6 Cell Viability .....	12
2.7 Establishing Hypoxia Model .....	13
2.8 Western Blotting.....	13
2.9 RNA-Seq Libraries Construction and Sequencing.....	14
2.10 Alignment and Analysis of Illumina Reads.....	15
2.11 Differential Gene Expression Analysis .....	16
2.12 Gene Set and Gene Ontology Enrichment Analyses .....	16
2.13 Protein-protein Interaction Networks .....	17
2.14 Quantitative Polymerase Chain Reaction .....	17

2.15 Statistical Analysis .....	18
Chapter 3: Results .....	19
3.1 Morphology Assessment .....	19
3.2 Cell Viability .....	20
3.3 HIF1- $\alpha$ Expression .....	21
3.4 PCA and Hierarchical Cluster Heatmaps .....	21
3.5 Differential Gene Expression Analysis .....	23
3.6 GSEA and GO Analysis .....	24
3.7 PPI Networks .....	32
3.8 Validation by qPCR .....	34
Chapter 4: Discussion .....	35
4.1 Effects of Hypoxia Mimicking-conditions .....	36
4.2 Effects of Stromal Signaling in 2D Microenvironment Model .....	38
4.3 Effects of Spatial Arrangement in 3D Culture .....	40
4.4 Modeling the Microenvironment of Liver Cancer .....	42
Chapter 5: Conclusion .....	49
References .....	50

## List of Tables

Table 1: RNA extraction quality control.....	15
Table 2: List of primers and their sequences .....	18
Table 3: List of the top 25 DEGs .....	24
Table 4: Enriched GSEA terms of DEGs.....	26
Table 5: Enriched GO terms associated with upregulated genes.....	28
Table 6: Enriched GO terms associated with downregulated genes.....	31
Table 7: Enriched GO terms associated with key regulators in group 5.....	33

## List of Figures

Figure 1: Schematic illustration of the TME .....	2
Figure 2: Role of hypoxia in the malignant process .....	5
Figure 3: Schematic illustration of liver cancer-microenvironment interactions .....	6
Figure 4: Spheroids recapitulate in vivo conditions.....	8
Figure 5: Schematic illustration of experimental design.....	9
Figure 6: Morphology assessment of 2D and 3D SV-80 cultures .....	19
Figure 7: Morphology assessment of 2D and 3D HepG2 cultures .....	20
Figure 8: Effects of CoCl <sub>2</sub> treatment on HepG2 cells .....	21
Figure 9: PCA plot and hierarchical cluster heatmap of all culturing conditions .....	22
Figure 10: Network of GO categories of upregulated genes in group 5 .....	29
Figure 11: Venn diagram and heatmap for genes of GO terms of interest .....	30
Figure 12: PPI network of multicellular organismal development genes .....	32
Figure 13: Validation by qPCR.....	34

## List of Abbreviations

2D	Two-dimensional
3D	Three-dimensional
AP-1	Activator protein 1
ATF-2	Activating Transcription Factor 2
ATM	Ataxia telangiectasia-mutated
CA9	Carbonic anhydrase 9
CAFs	Cancer-associated fibroblasts
CoCl <sub>2</sub>	Cobalt (II) Chloride hexahydrate
DEGs	Differentially expressed genes
DKK1	Dickkopf WNT signaling pathway inhibitor 1
DKK4	Dickkopf WNT signaling pathway inhibitor 4
ECM	Extracellular matrix
EGFR	epidermal growth factor receptor
EMT	Epithelial mesenchymal transition
FDR	False discovery rate
GC	Glucocorticoids
GCR	Glucocorticoids receptors
GO	Gene ontology
GSEA	Gene set enrichment analysis
HCC	Hepatocellular carcinoma
HDAC3	Histone deacetylase 3
HIF	Hypoxia-inducible factor
HIF1- $\alpha$	Hypoxia-inducible factor-1 alpha



HIF2- $\alpha$	Hypoxia-inducible factor-2 alpha
IL-6	Interleukin-6
MMPs	Matrix metalloproteinase
PCA	Principle component analysis
PFKFB3	6-Phosphofructo-2-Kinase/Fructose-2,6-Biphosphate 3
PPI	Protein-protein interactions
qPCR	Quantitative Polymerase Chain Reaction
ROS	Reactive oxygen species
SHP2	Src-homology 2 domain-containing phosphatase 2
STAT3	Signal transducer and activator of transcription 3
TME	Tumor microenvironment
TNS-1	Tensin-1

## **Chapter 1: Introduction**

### **1.1 The Tumor Microenvironment**

As a multistep disease, cancer cells arise from normal cells, through accumulation of mutations and acquiring a set of properties or hallmarks promoting their progression and survival. Douglas Hanahan and Robert Weinberg argued that most cancers, despite arising from different tissues, exhibit a universal set of hallmarks that underline their malignant transformation (Hanahan and Weinberg, 2000). The six hallmarks include evading cell death, prolong proliferative signaling, escaping growth suppression, inducing angiogenesis, enabling replicative immortality, and initiating invasion and metastasis. However, two additional hallmarks were subsequently added in the following years that included escaping of immune destruction and cancer cells reprogramming of their metabolism and energy production. This updated view also implicated the tumor microenvironment (TME) as a key player in cancer progression and acquisition of these cancer-supporting hallmarks (Hanahan and Weinberg, 2011; Wang et al., 2017).

Rapidly dividing cells represent only one player in the complex process of tumorigenesis. Tumor surroundings are composed of a dynamic network of non-malignant cellular components, non-cellular components, signaling molecules, and extracellular matrix (ECM) (Catalano et al., 2013; Quail and Joyce, 2013), which collectively form the tumor microenvironment (TME) (Figure 1). A two-way communication between the tumor and the surrounding dynamic network, TME, sustains and contributes to the growth and metastasis of the tumor (Hanahan and Weinberg, 2011). Such communication is underlined in an increasing body of evidence that highlights the key role played by the TME in tumor progression (Balkwill et al.,

2012; Klemm and Joyce, 2015; Quail and Joyce, 2013; Hanahan and Coussens, 2012); This communication is also well manifested through the ongoing signals that tumor sends to its highly responsive microenvironment to compose a supportive milieu (Quail and Joyce, 2013). In addition, many studies have reported the positive role of the TME in restraining tumor initiation and progression at initial stages of carcinogenesis (Bissell and Hines, 2011), and how “re-programming” the TME in the later stages holds great potential in terms of effective cancer treatments (Quail and Joyce, 2013).

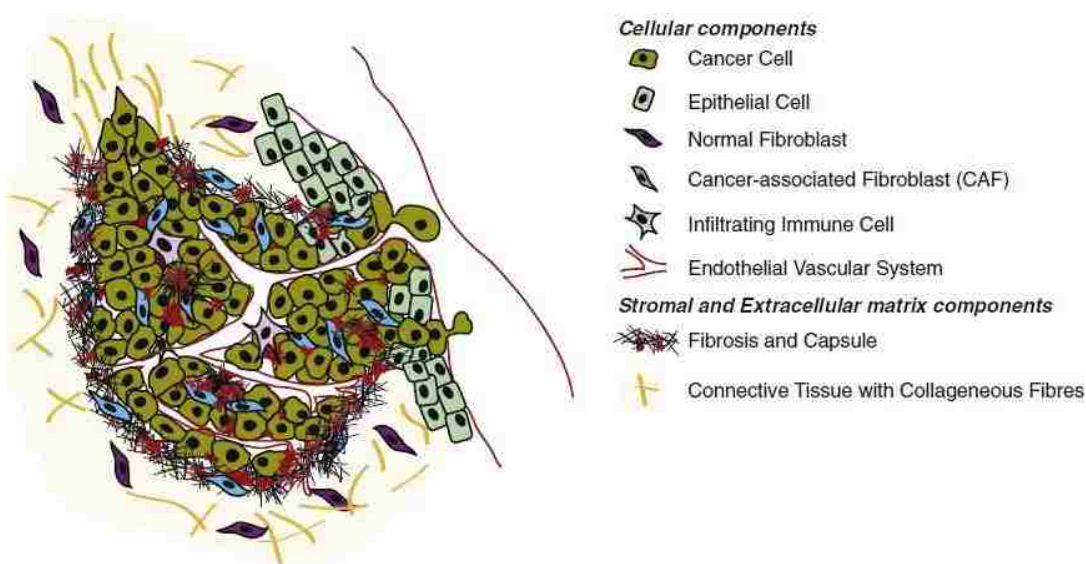


Figure 1: Schematic illustration of the TME. Cellular and non-cellular components surround cancer cells in the TME (Thoma et al., 2014).

## 1.2 Cancer Associated Fibroblasts

The most dominant cellular component of the TME are fibroblasts. Normally, these cells are in an “inactive” quiescent state; however, they get activated when wound healing and inflammation processes are triggered due to tissue damage (Marsh et al., 2013). After which, the activated population of fibroblasts undergo apoptosis, leaving only quiescent fibroblasts. However, this is not the case in tumorigenesis,

where activated fibroblasts do not undergo apoptosis (Marsh et al., 2013), and remain perpetually activated, leading in most cases to fibrosis (Wang et al., 2017). It has been suggested that fibroblasts that have been recruited to the tumor site are constantly activated by the tumor through paracrine signaling, after which they are transformed into cancer-associated fibroblasts (CAFs) (Öhlund et al., 2014). Once the CAF phenotype is set, paracrine signaling from the tumor is no longer needed to maintain the CAF transition (Orimo et al., 2005). These transformed fibroblasts are distinct in their morphology and function from normal fibroblasts (Orimo et al., 2005); they possess higher ability to proliferate (Kalluri and Zeisberg, 2006), are always present in the tumors' vicinity, and are capable of evading apoptosis (Cirri and Chiarugi, 2012).

CAFs contribute significantly to tumor growth and progression through several mechanisms that depends on the communication between CAFs and the tumor cells, and the communication among CAFs and other cellular components in the TME (Marsh et al., 2013). Indeed, the promoting role of CAFs in tumor progression functions through suppressing immune responses, secreting growth factors, cytokines, and proangiogenic factors (Zhang and Liu, 2013). In addition, CAFs contributes to tumorigenesis through secreting ECM proteins and the degrading matrix metalloproteinase (MMPs), which together, gives CAFs their ECM remodeling ability (Zhang and Liu, 2013). Collectively, such functional roles, among others, highlights the great potential in approaching CAFs as therapeutic targets.

### **1.3 Hypoxia**

As the tumor develops and keeps growing, it has a much higher demand on oxygen and nutrients to support its progression. Thus, survival of the tumor mass is highly

dependent on the formation of new blood vessels, or what is known as angiogenesis. Nonetheless, when the constant demand of oxygen by highly proliferative cancer cells is not met by the existing and the newly formed blood vessels, an area of low oxygen content is formed. Such areas experience much lower oxygen level than that of normal physiological conditions, and they are considered hypoxic (Span and Bussink, 2015). To survive the hostile conditions, tumor cells switch on different signaling pathways, that turn on hypoxia-inducible factor (HIF)-mediated gene expression (Span and Bussink, 2015). Under hypoxic conditions, HIF-1 is activated and, in turn, activates the transcription of a group of genes through binding to their hypoxia- response elements to promote the survival of the tumor cells (Brahimi-Horn et al., 2007). HIF-1 targeted genes significantly contribute to different aspects in tumor progression, such as angiogenesis, metastasis, adhesion, metabolism, and pH regulation (Brahimi-Horn et al., 2007). Moreover, many studies have highlighted the role of hypoxia in recruiting stroma components in the TME (Casazza et al., 2014; Semenza, 2013) and the association of hypoxia with ECM composition and remodeling to promote metastasis (Gilkes et al., 2014). A summary of hypoxia's role in tumor progression is shown in Figure 2.

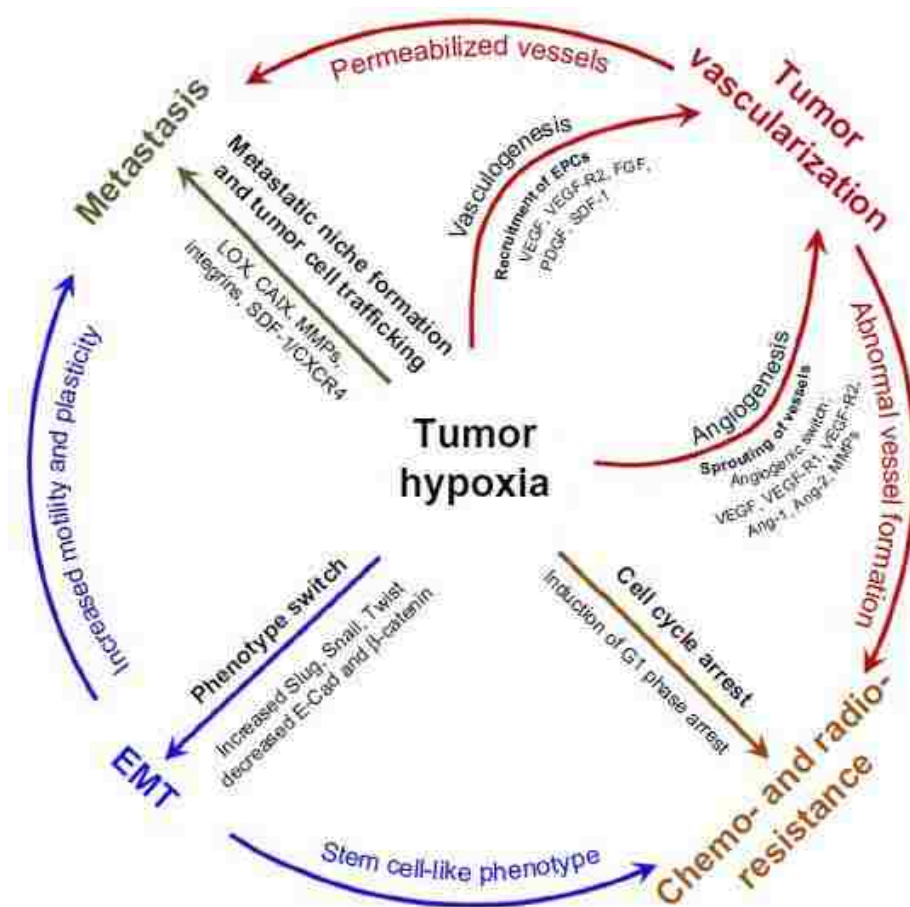


Figure 2: Role of hypoxia in the malignant process. Hypoxia drives tumor progression through promotion of pro-survival pathways such as angiogenesis, EMT, metastasis, and drug resistance (Muz et al., 2015).

#### 1.4 Hepatocellular Carcinoma

The fifth most common cancer globally is hepatocellular carcinoma (HCC), and it is the second cause of cancer-related death globally, where it accounted for about 746,000 deaths in 2012 alone (Ferlay et al., 2013). HCC has a very poor prognosis, it is usually diagnosed in late stages with very poor five-year survival rate (Ferlay et al., 2013).

There is an increasing support of the notion that HCC progression is highly influenced by elements in the liver microenvironment (Tu et al., 2014). Some of these elements that are driving HCC progression and tumor survival include altered stromal

cells (*i.e.* fibroblasts). As mentioned earlier, these cells are able to deposit ECM proteins, or what is known as fibrosis that then progresses to cirrhosis (Tu et al., 2014). 80%-90% of HCC patients experience cirrhosis, suggesting a crucial role of ECM build-up in HCC progression (Fattovich et al., 2004). As with other solid tumors, hypoxia represents a driving microenvironmental element of HCC progression, and it is associated with poor prognosis (Lin and Wu, 2015; Wong et al., 2014). HIF-mediated gene expression contributes to different aspects of HCC metastasis, such as epithelial mesenchymal transition (EMT) (Zhang et al., 2013), invasion of the ECM, and metastasis (Wilson et al., 2014). Nonetheless, our knowledge is limited when it comes to the way stromal cells (*i.e.* fibroblasts and CAF) interact with tumor cells and other components of the TME to promote HCC progression under hypoxic conditions (Casazza et al., 2014). A schematic illustration of liver cancer-microenvironment interactions is shown in Figure 3.

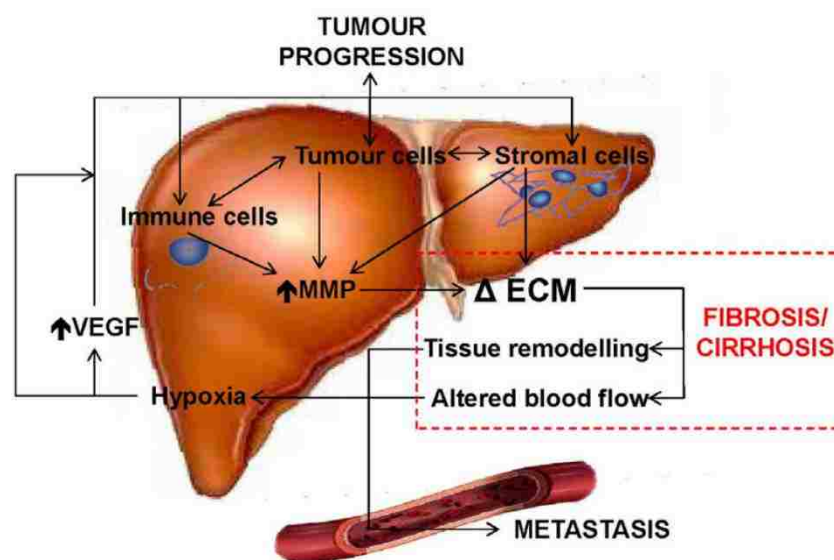


Figure 3: Schematic illustration of liver cancer-microenvironment interactions (Tu et al., 2014).

## 1.5 Three-dimensional Culture

To reflect the complexity and dynamicity of tumor biology, a physiologically relevant model is needed. This is even more stressed in the context of drug discovery and identifying effective therapeutic targets. To simulate *in vivo* environment, *in vitro* two-dimensional (2D) cell culture is typically utilized by growing cells on usually a plastic substrate in an adherent monolayer. However, such approach strips away many physiological parameter of the tumor. The distortion of spatial arrangement of cells in 2D culture changes cell-cell and cell-matrix interactions (Anton et al., 2015), and most importantly, alters the response of cells to certain drugs and treatments (Unger et al., 2014). Thus, utilizing three-dimensional (3D) cell culture models is needed to produce more biologically relevant platforms for understanding *in vivo* physiology. Indeed, 3D cultured cells are able to recapitulate *in vivo* architecture of tumors much better, and they are also able to exhibit a more similar gene expression to that of tumors *in vivo* (Anton et al., 2015). One very common 3D cultured cells model is the spheroid, which is a micro cell cluster that forms a sphere (Ingram et al., 1997). The nature of this model is what makes it an attractive tool to simulate solid tumors *in vitro* as it is composed of three regions, a highly proliferative outer region, a middle quiescent region, and a hypoxic core region (Ravi et al., 2015). Such compartmentalization creates a diffusional gradient of oxygen, nutrients, and exposure to drugs among all three regions of the spheroid, which is also characteristic of solid tumors (Mehta et al., 2012; Figure 4).



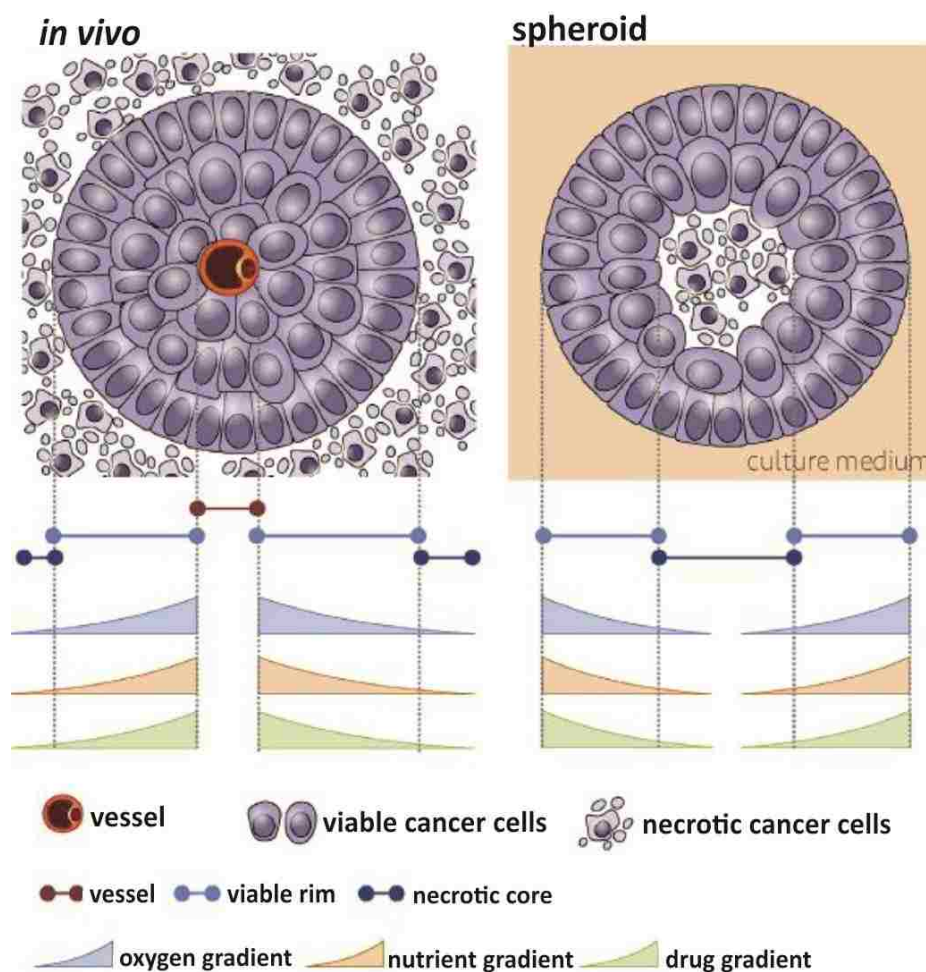


Figure 4: Spheroids recapitulate *in vivo* conditions. Gradients of oxygen, nutrients, and drug exposure form in spheroids, creating *in vivo* conditions *in vitro* (Stadler et al., 2015).

## 1.6 Hypotheses to be Tested

The aim of the study presented in this study is to create an *in vitro* model of liver cancer microenvironment using a 3D co-culture system of liver cancer cells with non-malignant fibroblasts. The hypothesis to be tested is based on three notions: A) if spatial organization affects function, and in consequence, malignancy? B) how does the crosstalk between the stroma and cancer cells affect progression and survival of cancer? C) does this model narrow the gap between conventional cell culture and the

living system? To address these questions, five experimental groups were established. Experimental design is shown in Figure 5.

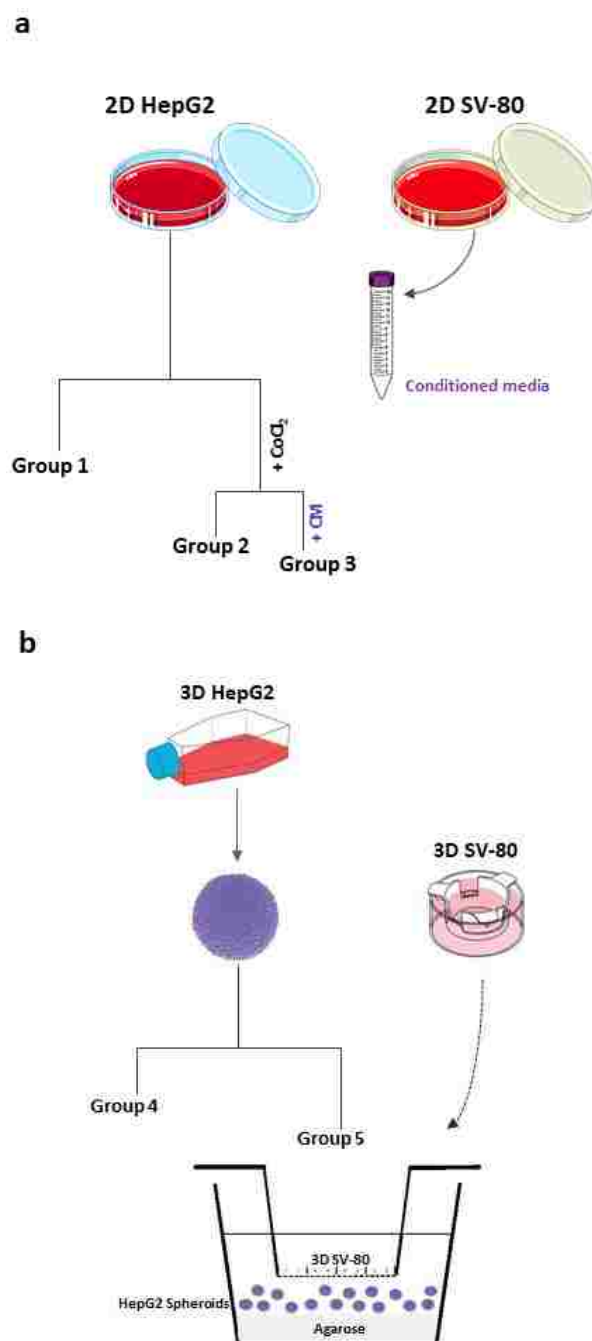


Figure 5: Schematic illustration of experimental design. a) preparation of 2D cultures (group 1, 2, and 3); and b) preparation of 3D cultures (group 4 and 5).

## **Chapter 2: Materials and Methods**

### **2.1 Cell Lines**

HepG2 (human Hepatoma cell line) and SV-80 (human fibroblast) were purchased from CLS (CLS GmbH, Germany). HepG2 and SV-80 cells were maintained in high-glucose DMEM medium supplemented with 10% FBS and 1% antibiotic/ antimycotic cocktail (HyClone, UK) at 37°C in 5% CO<sub>2</sub> humidified incubator. Cells were sub-cultured every 2-4 days using trypsin 0.25%.

### **2.2 2D Cell Culture**

For 2D mono-cultures, HepG2 and SV-80 cells were cultured at a density of  $1 \times 10^6$  in conventional 2D culturing flasks in DMEM media. Flasks were incubated at 37°C in 5% CO<sub>2</sub> humidified incubator.

### **2.3 3D Cell Culture**

For generation of HepG2 spheroids, HepG2 cells were trypsinized and resuspended as single cell suspension before being seeded at  $1 \times 10^6$  cell density in Corning® Ultra-Low attachment cell culture flasks coated with poly-HEMA (Corning, USA) to facilitate spheroid formation. Plates were incubated at 37°C in 5% CO<sub>2</sub> humidified incubator and spheroid formation was monitored using inverted microscopy.

For generation of 3D culture of fibroblasts, Alvetex strata inserts (Reinervate, UK) were used. SV-80 cells were trypsinized and resuspended as single cell suspension for cell counting. Alvetex inserts were prepared prior to cell seeding by three washes (1<sup>st</sup>: 70% ethanol, 2<sup>nd</sup>: growth media, 3<sup>rd</sup>: growth media). Inserts were

placed in 6-well plate and SV-80 cells were seeded in the Alvetex inserts in a density of  $1 \times 10^6$ .

## 2.4 Morphology Assessment

To study the morphological differences between 2D and 3D cultures, HepG2 and SV-80 cells were seeded in 8-well chambers for 2D culture; or in ULA plates and Alvetex inserts, respectively, for 3D culture. 2D cultures of HepG2 and SV-80 were seeded at a density of  $2 \times 10^4$  and  $1 \times 10^4$  cells/ well in an 8-well chamber, respectively. They were fixed with 100% methanol and stained with crystal violet. 3D culture of HepG2 was seeded at a density of  $1 \times 10^6$  and monitored over a period of 5 days. Spheroids were harvested, fixed, and stained with crystal violet and immobilized on agarose pads for imaging. 3D culture of SV-80 was seeded at a density of  $0.5 \times 10^6$ , then fixed and stained with neutral red. Inserts were unclipped and scaffolds were placed on glass slides for imaging using IX53 inverted microscope (Olympus, Japan).

In addition, immunofluorescence was utilized to better visualize the difference between SV-80 2D and 3D cultures. Cultures were washed with ice-cold 1X PBS, fixed with pre-chilled methanol for 10 minutes at  $-20^\circ\text{C}$ , permeabilized with 0.5% Triton X-100 PBS, and blocked with 1% BSA solution (in 0.5% Triton X-100 PBS) for 30 minutes at room temperature. Cells were incubated with primary antibody against  $\alpha$ -Tubulin (1:100; ab176560) overnight at  $4^\circ\text{C}$ , then incubated with Alexa Fluor® 488- conjugated secondary antibody (1:200) for 1 hour at room temperature, and counterstained with DAPI. Antibodies were diluted in 1% BSA. Images were taken using IX53 inverted microscope (Olympus, Japan).

## 2.5 Co-culture Systems

For the 2D co-culture, a one-way communication system was followed. Briefly, HepG2 and SV-80 cells were seeded at a density of  $1 \times 10^6$  in conventional 2D culturing flasks in DMEM media. Flasks were incubated at 37°C in 5% CO<sub>2</sub> humidified incubator for about 24 hours. Conditioned media of SV-80 cell line was collected, centrifuged to collect any cellular debris, and applied to HepG2 cells, which were incubated with the conditioned media for 48 hours.

For the 3D co-culture, a two-way communication system was followed. Briefly, HepG2 and SV-80 3D cultures were prepared separately. Prior to co-culture, 6-well plates were coated with 1.5% agarose, and allowed to set and cool before transferring HepG2 spheres to the bottom of the coated plates, and the inserts containing SV-80 3D culture were placed on top. HepG2 and SV-80 3D cultures were incubated for 48 hours.

## 2.6 Cell Viability

To assess the effects of hypoxia-mimetic agent CoCl<sub>2</sub> on cellular viability, HepG2 cells were seeded at a density of  $5 \times 10^3$  cells/ well in a 96-well plate. Cells were allowed to attach prior to treatment with increasing concentrations of CoCl<sub>2</sub> (100-400 μM). Cell viability was assessed using CellTiter-Glo Luminescent Assay (Promega, USA), according to manufacturer instructions. Luminescent signals were recorded using GloMax Discover (Promega, USA). The experiment was repeated three times (n=12).

## 2.7 Establishing Hypoxia Model

To mimic the hypoxic microenvironment, 2D cultures of HepG2 cells were cultured as previously described in section 2.2 and treated with 200 and 300  $\mu\text{M}$  of Cobalt (II) Chloride hexahydrate ( $\text{CoCl}_2$ ) for 6 hours prior to harvesting. The doses and incubation time are based on literature demonstrating HIF1- $\alpha$  maximum induction at 4-6 hours of  $\text{CoCl}_2$  treatment, over a range of doses (Liu et al., 2015). Under normoxia, HIF1- $\alpha$  protein is degraded, and hence, serves as a marker for hypoxia. Western blot was carried out to assess expression of HIF1- $\alpha$  in  $\text{CoCl}_2$  treated and non-treated cells.

## 2.8 Western Blotting

Cells were harvested in ice-cold PBS and then lysed with appropriate volume of RIPA buffer containing phosphatase and protease inhibitor and incubated on ice for 30 minutes, vortexing every 10 minutes. Samples were centrifuged at 12000 rpm for 30 minutes at 4°C. The pellet was discarded, and the supernatant was transferred to a new tube for protein quantification using BCA assay. Total protein was separated with 8% SDS-PAGE. After running the gel, proteins were transferred to a PVDF membrane that was then blocked with 5% non-fat dry milk TBST for 1 hour at room temperature. Membranes were incubated with primary antibody against HIF1 $\alpha$  (H1alpha67, ChIP grade) at 1:200 dilution, GAPDH (ab181602) at 1:40000 dilution overnight at 4°C. All primary antibodies were diluted in 2% non-fat dry milk TBST. Membranes were washed with TBST and then incubated with secondary antibodies against HIF1 $\alpha$  (anti-mouse, 7076s) at 1:1000 dilution, and against GAPDH (anti-rabbit, 7074s cell signal) at 1:1000 dilution for 1 hour at room temperature. All secondary antibodies were diluted in 2% non-fat dry milk TBST. Blots were then visualized using LI-COR C-

DiGit Blot Scanner. Quantification of visualized bands was performed using ImageJ software.

## **2.9 RNA-Seq Libraries Construction and Sequencing**

For RNA extraction, all groups were prepared as described previously, then collected, washed with 1X PBS, and resuspended in RNAlater stabilization solution before storing at -80°C. Total RNA was isolated from three biological replicates of all groups using RNeasy Mini Kit (Qiagen) following manufacturer's instructions. Concentration and purity of total RNA was assessed using NanoDrop2000. Quality control of RNA samples was performed with Agilent 2100 Bioanalyzer RNA 6000 Nano Kit, concentrated samples were diluted with RNase-free water prior to bioanalyzer run. Purity scores and RINs for all groups are listed in Table 1.

The RNAseq libraries were prepared by DNA Sequencing Center in Brigham Young University. Briefly, KAPA Stranded mRNA-Seq Kit (Kapa Biosystems, USA) was used for capturing poly(A) RNA, converting it to cDNA, A-tailing, and Adapter ligation. Fragments carrying appropriate adapter sequences were amplified to yield mRNA-Seq libraries. KAPA Library Quantification Kit (Kapa Biosystems, USA) was used for libraries quantification prior to Illumina sequencing using high-throughput Illumina HiSeq sequencing system (Illumina, USA).

	260/280	RIN
Group 1	2.10	10
Group 1'	2.11	10
Group 1''	2.10	10
Group 2	2.06	10
Group 2'	2.10	10
Group 2''	2.10	10
Group 3	2.10	10
Group 3'	2.07	10
Group 3''	2.08	10
Group 4	2.09	10
Group 4'	2.09	10
Group 4''	2.08	10
Group 5	2.07	10
Group 5'	2.10	10
Group 5''	2.09	10

Table 1: RNA extraction quality control. 260/280 ratio and RINs for all groups obtained from NanoDrop 2000 and Agilent 2100 Bioanalyzer.

## 2.10 Alignment and Analysis of Illumina Reads

Briefly, reads obtained from Illumina were aligned to Homo sapiens GRCh38.p2 reference genome using tophat2 v2.1.0. Following alignment and annotation, read counts were generated using HTseq count. Alignment and generation of read counts were performed by NYU-AD bioinformatics core.

Read counts were used to generate principle component analysis (PCA) plot and hierarchical cluster heatmaps, using the web-based tool ClustVis ([https://biit.cs.ut.ee/clustvis\\_large/](https://biit.cs.ut.ee/clustvis_large/)), for clustering of multivariate data. Triplicates of each group are collapsed by taking the mean, and rows were scaled using vector scaling method. Due to limitation on input data size, 2400 genes were selected randomly for generation of heatmap in Figure 11.



### 2.11 Differential Gene Expression Analysis

RNA-seq 2G (<http://52.90.192.24:3838/rnaseq2g/>) was used to perform analysis of differential gene expression using read counts between group 1 (2D HepG2 under normoxia), group 2 (2D HepG2 treated with CoCl<sub>2</sub>), group 3 (2D co-culture HepG2 treated with CoCl<sub>2</sub>), group 4 (3D HepG2), and group 5 (3D co-culture HepG2). Counts were normalized using DEseq method, and differential expression was determined using DEseq2 method. Obtained DEGs with false discovery rate (FDR) <0.05 and exhibiting a fold change  $\leq -2$  and  $\geq 2$  were identified as significant DEGs.

### 2.12 Gene Set and Gene Ontology Enrichment Analyses

Gene set enrichment analysis (GSEA) was carried on sets of upregulated and downregulated genes using canonical pathways ontology on eXploring Genomic Relations (XGR) web version (<http://galahad.well.ox.ac.uk:3020/enricher/genes>). Enriched terms were tested for significance using the Hypergeometric test, and only terms with FDR < 0.05 were considered. Gene ontology (GO) enrichment analysis was carried out using Biological Networks Gene Ontology (BiNGO) App (Maere et al., 2005) in Cytoscape, an open source software platform for network data integration, analysis, and visualization (Killcoyne et al., 2009). Based on Hypergeometric significance test, corrected multiple testing using Benjamini and Hochberg FDR < 0.05, and using biological process ontology, relevant enriched terms were identified by BiNGO.

InteractiVenn (<http://www.interactivenn.net/>) was used to generate a Venn diagram of relevant GO terms by uploading sets of their associated genes (Heberle et al., 2015).

### 2.13 Protein-protein Interaction Networks

The web platform Network Analyst (<http://www.networkanalyst.ca/>) was used to generate protein-protein interaction (PPI) networks. By providing a list of genes with their corresponding log fold changes, PPI networks were generated based on STRING Interactome with confidence score cutoff of 700 (1000 being highest) and required experimental evidence (Xia et al., 2014). Modules were identified using module explorer function; modules with highest connections were selected for further analysis.

### 2.14 Quantitative polymerase chain reaction

For the purpose of validating genes of interest, quantitative polymerase chain reaction (qPCR) was carried out on samples from groups 1 and 5. Total RNA was converted to cDNA using GoScript™ Reverse Transcription System, according to manufacturer's instruction (Promega, USA). GoTaq® qPCR Master Mix (Promega, USA) was used to perform qPCR on QuantStudio 5 Real-Time PCR System (Applied Biosystems, USA) using gene-specific primers purchased from Macrogen (Macrogen Inc., South Korea). 18S rRNA was used for data normalization due to its unchanged expression in groups 1 and 5. Comparative C<sub>T</sub> method ( $2^{-\Delta\Delta C_T}$ ) was used to determine fold change in expression of target genes between group 5 and group 1 (Schmittgen and Livak, 2008), according to the following equation:

$$2^{-\Delta\Delta C_T} = [(C_T \text{ gene of interest} - C_T \text{ internal control}) \text{ group 5} - (C_T \text{ gene of interest} - C_T \text{ internal control}) \text{ group 1}]$$

The cycling parameters recommended in GoTaq® qPCR Master Mix manual were used. Briefly, Hot-Start Activation was carried at 95°C for 2 minutes, 40 cycles of denaturation at 95°C for 15 seconds, followed by annealing/ extension at 60°C for 60 seconds, and then dissociation at 60–95°C. All reactions were carried in triplicates, and primers sequences are shown in Table 2.

Primer	Forward (5'→3')	Reverse (5'→3')	Source
CA9	CATCCTAGCCCTGGTTTTGG	GCTCACACCCCCTTTGGTT	Beucken et al., 2009
PFKFB3	ATTGCGGTTTTCGATGCCAC	GCCACAACCTGTAGGGTCGT	Primer Bank: 223941849c2
SERPINE1	CAACTTGCTTGGGAAAGGAG	GGGCGTGGTGAACCTCAGTAT	Xu et al., 2015
ETS1	TTCACTAAAGAACAGCAAC	TGTCCCCAACAAAGTCTG	Zheng et al., 2013
MMP3	TGGCATTGAGTCCCTCTATGG	AGGACAAAGCAGGATCACAGTT	RTPrimer Database: 3211
MMP7	ATGTGGAGTGCCAGATGTTGC	AGCAGTTCCCCATACAACCTTC	Primer Bank: 75709180c2
E2F2	CGTCCCTGAGTTCCCAACC	GCGAAGTGTGATACCGAGTCTT	Primer Bank: 315075284c1
E2F7	CTCCTGTGCCAGAAGTTC	CATAGATGCGTCTCCTTTCC	Weijts et al., 2012
E2F8	AATATCGTGTGGCAGAGATCC	AGGTTGGCTGTCGGTGTGTC	Weijts et al., 2012
18S rRNA	AGTCCCTGCCCTTTGTACACA	GATCCGAGGGCCTCACTAAAC	Beucken et al., 2009

Table 2: List of primers and their sequences

## 2.15 Statistical Analysis

Statistical analysis was performed using GraphPad Prism 7 and Microsoft Excel. Two-tailed, paired t-test was used to analyze the data, where statistical significance was assumed at  $p < 0.01$ . Data is represented as mean  $\pm$  SD.

## Chapter 3: Results

### 3.1 Morphology Assessment

HepG2 and SV-80 cells were cultured in 2D and 3D systems to examine the morphological changes accompanying the changes in the culturing environment. SV-80 cells grown as a 2D culture exhibit an elongated morphology. However, growing SV-80 as 3D culture in porous scaffolds alters their morphology entirely. By forcing them to grow within the pores of the scaffold, SV-80 cells are no longer elongated, instead they exhibit a round morphology and a smaller size than their 2D counterparts (Figure 6).

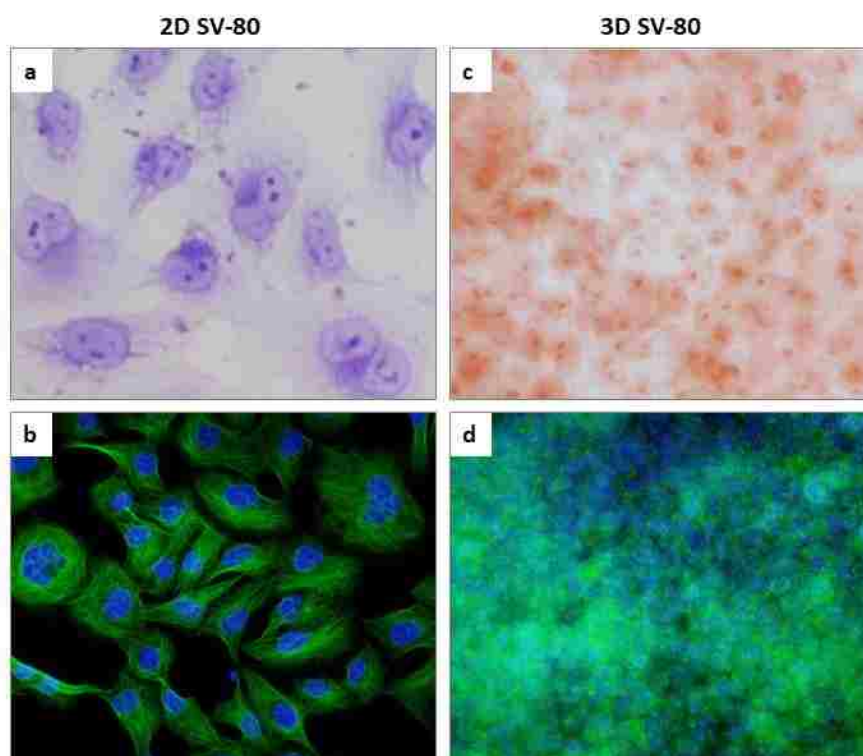


Figure 6: Morphology assessment of 2D and 3D SV-80 cultures. a) Brightfield image of 2D SV-80 fixed and stained with crystal violet (40X). b) Fluorescence image of 2D SV-80 fixed and incubated with anti-Tubulin primary antibody and Alexa Fluor 488-conjugated secondary antibody (green), and counterstained with DAPI (20 X). c) Brightfield image of 3D SV-80 fixed and stained with neutral red (40X). d) Fluorescence image of 3D SV-80 fixed and incubated with anti-Tubulin primary antibody and Alexa Fluor 488- conjugated secondary antibody (green), and counterstained with DAPI (40 X).

On the other hand, HepG2 grown as a 2D culture forms clusters or islands on the plastic culturing surface. HepG2 cells grown in 3D were monitored over a period of 5 days to assess formation of tightly aggregated spheroids. Starting at the second day, HepG2 cells started forming tight aggregates, whereas by the fourth day HepG2 started forming tight spheroids with a smooth surface (Figure 7).

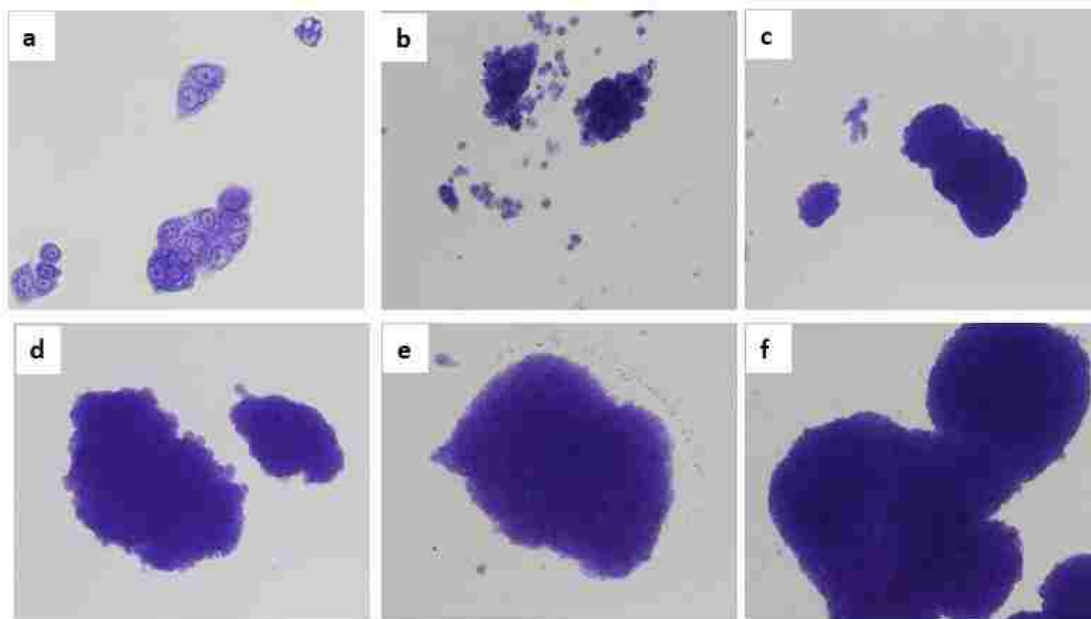


Figure 7: Morphology assessment of 2D and 3D HepG2 cultures. a) Brightfield image of 2D HepG2 fixed and stained with crystal violet at day 3 (20 X). b) Brightfield image of 3D HepG2 fixed and stained with crystal violet at day 1, c) at day 2, d) at day 3, e) at day 4, f) at day 5 (10 X).

### 3.2 Cell Viability

HepG2 2D cultures were treated with increasing concentrations of  $\text{CoCl}_2$  (100-400  $\mu\text{M}$ ) to assess cellular viability under hypoxia-mimicking conditions. Treatment of HepG2 with  $\text{CoCl}_2$  did not alter cellular viability in a significant manner at doses of 100 and 200  $\mu\text{M}$  of  $\text{CoCl}_2$ . However, a significant difference ( $p < 0.01$ ) was noted at doses of 300 and 400  $\mu\text{M}$  of  $\text{CoCl}_2$  (Figure 8 a).

### 3.3 HIF1- $\alpha$ Expression

To confirm the induction of hypoxia in CoCl<sub>2</sub>- treated HepG2 2D cultures, protein expression of HIF1 $\alpha$  was assessed using western blot. As shown in Figure 8 b, treatment with 200  $\mu$ M of CoCl<sub>2</sub> for 6 hours did not induce HIF1 $\alpha$  expression. However, by increasing the dose to 300  $\mu$ M, HIF1 $\alpha$  expression was detected in HepG2 cells.

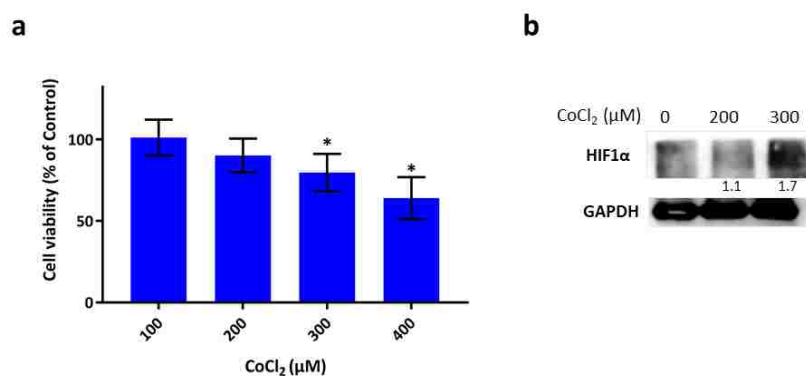


Figure 8: Effects of CoCl<sub>2</sub> treatment on HepG2 cells. a) Cell viability of HepG2 cells after treatment with increasing concentrations of CoCl<sub>2</sub> for 6 hours ( $p < 0.01$ ). b) HIF1- $\alpha$  protein expression was detected in CoCl<sub>2</sub> HepG2-treated cells after 6 hours of incubation. Protein bands were quantified using ImageJ software. Each band intensity was quantified using ImageJ, normalized relative to their respective loading control bands, then treated groups are expressed as a ratio of control.

### 3.4 PCA and hierarchical cluster heatmaps

PCA was used to explore how different culturing conditions translate into changes in global gene expression. In a PCA plot, groups exhibiting similarity will cluster closer together than those with less similarity. As shown in Figure 9 a, all the groups are gathered at the opposite extreme of the proposed model (group 5), where the conventional HepG2 culture (group 1) is the furthest. A Heatmap was utilized to better visualize the expression of genes among different groups, and how groups will cluster together based on their expression profiles (Figure 9 b). Clustering rows (genes) and columns (groups) yielded a similar result to that of PCA, where group 5 clustered

separately from the rest of the groups. On the other hand, group 4 clustered with group 3, and group 2 clustered with group 1.

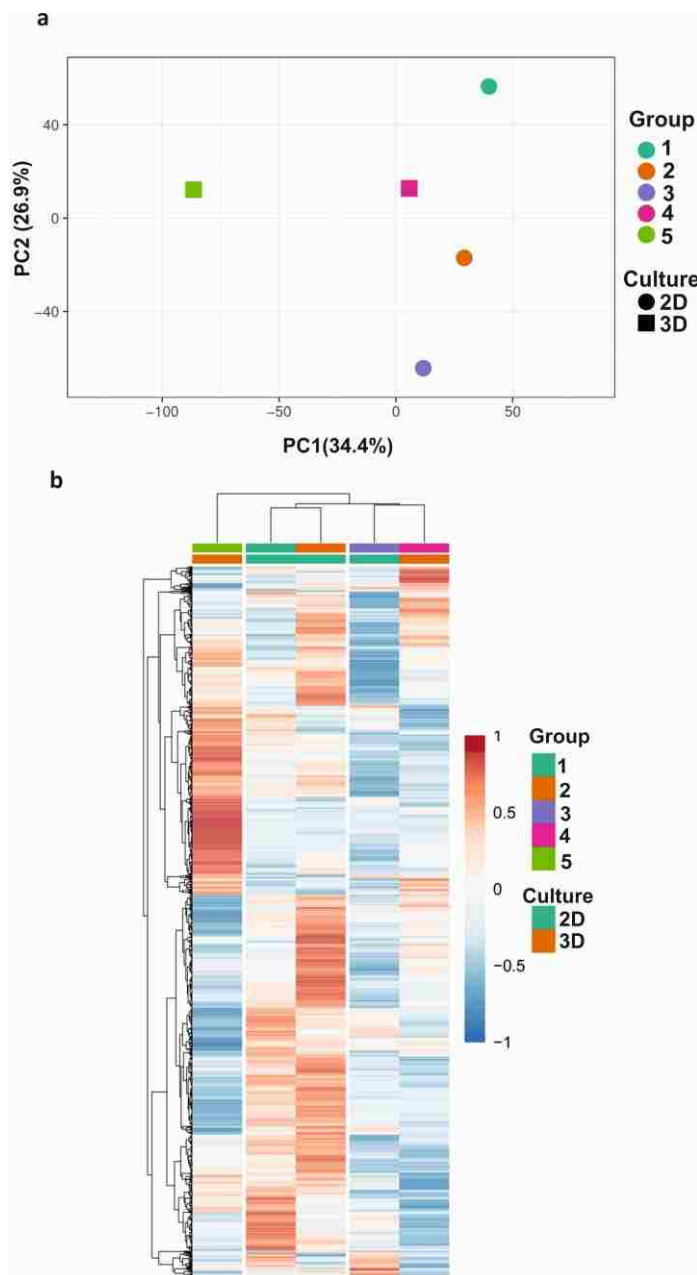


Figure 9: PCA plot and hierarchical cluster heatmap of all culturing conditions. a) PCA plot of all groups where triplicates of each group are collapsed by taking mean inside each group. Vector scaling is applied to rows; Nipals PCA is used to calculate principal components. X and Y axis show principal component 1 and principal component 2 that explain 34.4% and 26.9% of the total variance, respectively. b) Heatmap of all groups where triplicates of each group are collapsed by taking mean inside each group. Rows are centered; vector scaling is applied to rows. Rows are clustered using correlation distance and average linkage. Columns are clustered using Manhattan distance and single linkage. 2400 rows, 5 columns.

### 3.5 Differential gene expression analysis

Global gene expression profiles of different groups were compared to investigate the contribution of culturing conditions to gene expression. Significant differentially expressed genes (DEG) were determined relative to HepG2 2D-culture under normoxia (group 1). Culturing HepG2 cells under hypoxia-mimicking conditions (group 2) resulted in significantly upregulating 243 genes and downregulating 131 genes. Culturing 2D HepG2 cells with SV-80 fibroblasts under hypoxia-mimicking conditions (group 3) resulted in increasing the number of significantly DEGs to 474 upregulated and 145 downregulated genes. When comparing gene expression profile of HepG2 spheroids (group 4) to that of group 1, 203 genes were significantly upregulated, whereas 82 genes were downregulated. Co-culturing HepG2 spheroids with SV-80 cells grown in 3D culture (group 5) by far resulted in changing the gene expression of HepG2 by significantly upregulating 1291 and downregulating 880 genes in group 5 in comparison to group 1.

When looking at the top 100 upregulated genes, certain genes were found to overlap between groups. For example, 6-Phosphofructo-2-Kinase/Fructose-2,6-Biphosphatase 3 (PFKFB3) is in the top 5 upregulated genes in groups 2, 3, and 5, and in the top 50 in group 4. Carbonic anhydrase 9 (CA9) is the top upregulated gene in groups 4 and 5, in the top 5 in group 3 and in the top 55 in group 2. Tensin-1 (TNS1) is in the top 5 upregulated genes in group 5, in the top 10 in group 3, in the top 20 in group 4, in the top 65 in group 2. In contrast, top 100 downregulated genes did not exhibit overlapping trend among different groups. For example, Dickkopf WNT signaling pathway inhibitor 1 (DKK1) is the top downregulated gene in group 2, and in the top 10 in group 3; whereas it is not among the DEGs in group 4 and it is ranked the 879<sup>th</sup> (out of 880) downregulated gene in group 5. Similarly, E2F transcription



factors E2F2, E2F7, and E2F8 are in the top 25 downregulated genes in group 5, but were not among group 2 and 3 did not exhibit notable downregulation in comparison to group 1. List of the top 25 up- and down- regulated genes can be found in Table 3.

Group 2 UR	Group 2 DR	Group 3 UR	Group 3 DR	Group 4 UR	Group 4 DR	Group 5 UR	Group 5 DR
<i>PFKFB3</i>	<i>DKK1</i>	<i>PFKFB3</i>	<i>KLF15</i>	<i>CA9</i>	<i>PLG</i>	<i>CA9</i>	<i>PKI55</i>
<i>HMOX1</i>	<i>EGR1</i>	<i>CA9</i>	<i>ANKRD1</i>	<i>TNNI2</i>	<i>ALDH1L2</i>	<i>EGLN3</i>	<i>FAM111B</i>
<i>HSPA1A</i>	<i>KLF15</i>	<i>PLA2G2A</i>	<i>HIF0</i>	<i>SLC12A3</i>	<i>MID1IP1</i>	<i>TNS1</i>	<i>ARSI</i>
<i>HSPA1B</i>	<i>C8orf4</i>	<i>HMOX1</i>	<i>FGFR2</i>	<i>GPX3</i>	<i>TAGLN</i>	<i>PFKFB3</i>	<i>POLQ</i>
<i>PFKFB4</i>	<i>FOXQ1</i>	<i>ADM</i>	<i>C8orf4</i>	<i>SPAG4</i>	<i>FBLN5</i>	<i>NDRG1</i>	<i>E2F2</i>
<i>ADM</i>	<i>SOX9</i>	<i>PFKFB4</i>	<i>CDH5</i>	<i>SFRP5</i>	<i>GAS7</i>	<i>CYP1A1</i>	<i>SKIDA1</i>
<i>HSPA1B</i>	<i>JRK</i>	<i>EGLN3</i>	<i>DKK1</i>	<i>NDRG1</i>	<i>SPINK1</i>	<i>HK1</i>	<i>ANGPTL1</i>
<i>ARRDC3</i>	<i>ARSI</i>	<i>MATN3</i>	<i>SALL1</i>	<i>LCN15</i>	<i>NES</i>	<i>PNCK</i>	<i>GEN1</i>
<i>DNAJB4</i>	<i>CCDC71</i>	<i>TNS1</i>	<i>HAMP</i>	<i>PFKFB4</i>	<i>ANKRD1</i>	<i>AQP3</i>	<i>LGR5</i>
<i>NDRG1</i>	<i>ANKRD1</i>	<i>PPFIA4</i>	<i>TNFSF4</i>	<i>PNCK</i>	<i>AFP</i>	<i>MUC13</i>	<i>AC099344.2</i>
<i>SERPINE1</i>	<i>TNFSF4</i>	<i>NDRG1</i>	<i>SHC3</i>	<i>CHST15</i>	<i>GALNT13</i>	<i>NDUFA4L2</i>	<i>DGAT2</i>
<i>GABARAPL1</i>	<i>HIF0</i>	<i>FAM13A</i>	<i>FOXQ1</i>	<i>AC007319.1</i>	<i>DHRS2</i>	<i>SOCS3</i>	<i>E2F8</i>
<i>FAM13A</i>	<i>LINC01124</i>	<i>SERPINE1</i>	<i>ALDH1L2</i>	<i>NDUFA4L2</i>	<i>GS1309P15.2</i>	<i>FAM13A</i>	<i>RP11701H24.3</i>
<i>RP1145A17.4</i>	<i>TCF23</i>	<i>HSPA1A</i>	<i>MOGAT2</i>	<i>SMIM3</i>	<i>MAP1B</i>	<i>PPFIA4</i>	<i>RP11566E18.1</i>
<i>TNFSF9</i>	<i>KCNJ10</i>	<i>C1R</i>	<i>NR1H4</i>	<i>CD36</i>	<i>LINC01314</i>	<i>A4GALT</i>	<i>SHC3</i>
<i>GCLM</i>	<i>FOXJ1</i>	<i>HSPA1B</i>	<i>CASC10</i>	<i>ANGPTL1</i>	<i>LINC00958</i>	<i>G6PC</i>	<i>CXCL5</i>
<i>KDM3A</i>	<i>SLC6A14</i>	<i>SOCS3</i>	<i>RBP2</i>	<i>RNASET2</i>	<i>SLIT1</i>	<i>HSPA6</i>	<i>GFOD1</i>
<i>OSGIN1</i>	<i>PPP2R2C</i>	<i>GABARAPL1</i>	<i>ZNF512B</i>	<i>STRA6</i>	<i>SCARA3</i>	<i>ADM</i>	<i>SPTBN2</i>
<i>HSPA1B</i>	<i>TMEM147AS1</i>	<i>TNFSF9</i>	<i>SKIDA1</i>	<i>G6PC</i>	<i>SLC7A11</i>	<i>HCAR2</i>	<i>CGNL1</i>
<i>EGLN3</i>	<i>TNFAIP3</i>	<i>RIMKLA</i>	<i>USP2</i>	<i>TNS1</i>	<i>PLAGL1</i>	<i>IGFBP1</i>	<i>CTC-429P9.5</i>
<i>RIMKLA</i>	<i>KCTD21AS1</i>	<i>CD24</i>	<i>TCF23</i>	<i>TUBB1</i>	<i>CDH5</i>	<i>PCK1</i>	<i>RP11-121C2.2</i>
<i>ABHD4</i>	<i>RFXPAP</i>	<i>CHST15</i>	<i>ADH4</i>	<i>COL2A1</i>	<i>THBS1</i>	<i>GADD45B</i>	<i>PRIMA1</i>
<i>UBC</i>	<i>BIRC3</i>	<i>HSPA1B</i>	<i>AKNA</i>	<i>ODAM</i>	<i>RP1-140K8.5</i>	<i>RP51120P11.1</i>	<i>E2F7</i>
<i>BNIP3L</i>	<i>TIGD2</i>	<i>SIT1</i>	<i>TBX2</i>	<i>SLC28A1</i>	<i>UGT2B4</i>	<i>ARRDC3</i>	<i>DUXAP9</i>
<i>DEDD2</i>	<i>ZNF385B</i>	<i>FOS</i>	<i>GATA2AS1</i>	<i>APOC3</i>	<i>AREG</i>	<i>SERPINE1</i>	<i>SPTLC3</i>

Table 3: List of the top 25 DEGs. Top up- (UR) and down-regulated (DR) genes in groups 2, 3, 4, and 5 in comparison to group 1.

### 3.6 GSEA and GO Analysis

To gather more insights into the function of the DEGs among different culturing conditions, XGR and BiNGO were used to identify enrichment terms in canonical pathways and biological processes, respectively.

GSEA was performed using XGR on all significant DEG in different culturing conditions. Upregulated genes due to culturing HepG2 cells under hypoxia-mimicking conditions (group 2) resulted in upregulating genes involved in hypoxia-inducible

factor-1 alpha (HIF1- $\alpha$ ), hypoxia-inducible factor-2 alpha (HIF2- $\alpha$ ), activator protein 1 (AP-1), and Activating Transcription Factor 2 (ATF-2) networks; among other pathways. GSEA revealed that the downregulated genes under hypoxia encode secreted soluble factors, and extracellular matrix (ECM) associated proteins (Table 4). Similarly to group 2, culturing HepG2 cells with SV-80 fibroblasts under hypoxia-mimicking conditions (group 3) upregulated genes involved in HIF1 $\alpha$ , HIF2 $\alpha$ , AP-1, and ATF-2 networks. In addition, upregulated genes in group 3 are involved in integrin family cell surface interactions, interleukin-6 (IL6) mediated signaling events, and remodeling of the extracellular matrix; whereas downregulated genes are involved in Wnt/  $\beta$ -catenin pathways (Table 4). Interestingly, 3D culturing of HepG2 (group 4), without treatment with hypoxia-mimicking agent CoCl<sub>2</sub>, upregulated genes involved in HIF1 $\alpha$  and HIF2 $\alpha$  transcription factor networks (Table 4).

Term Name	FDR
<b>Group 2 UR</b>	
HIF-1-alpha transcription factor network	5.30E-11
Direct p53 effectors	6.40E-07
HIF-2-alpha transcription factor network	1.60E-04
AP-1 transcription factor network	1.10E-03
Validated transcriptional targets of deltaNp63 isoforms	4.70E-03
ATF-2 transcription factor network	1.10E-02
<b>Group 2 DR</b>	
Genes encoding secreted soluble factors	1.40E-02
Ensemble of genes encoding ECM-associated proteins including ECM-affiliated proteins, ECM regulators and secreted factors	2.80E-02
<b>Group 3 UR</b>	
HIF-1-alpha transcription factor network	6.20E-15
Beta1 integrin cell surface interactions	1.00E-08
uPA and uPAR-mediated signaling	8.90E-06
Beta3 integrin cell surface interactions	8.90E-06
HIF-2-alpha transcription factor network	5.40E-05
Genes encoding enzymes and their regulators involved in the remodeling of the extracellular matrix	5.40E-05
IL6-mediated signaling events	6.90E-04
AP-1 transcription factor network	7.60E-03
Validated transcriptional targets of deltaNp63 isoforms	9.60E-03
Cytokines can induce activation of matrix metalloproteinases, which degrade extracellular matrix.	9.60E-03
<b>Group 3 DR</b>	
Wnt/beta-catenin Pathway	3.10E-04
Genes related to Wnt-mediated signal transduction	8.80E-04
<b>Group 4 UR</b>	
HIF-1-alpha transcription factor network	8.40E-11
Ensemble of genes encoding extracellular matrix and extracellular matrix-associated proteins	3.30E-04
Genes encoding enzymes and their regulators involved in the remodeling of the extracellular matrix	7.60E-04
Ensemble of genes encoding ECM-associated proteins including ECM-affiliated proteins, ECM regulators and secreted factors	1.20E-03
HIF-2-alpha transcription factor network	3.50E-03
<b>Group 4 DR</b>	
Glucocorticoid receptor regulatory network	4.00E-02
<b>Group 5 UR</b>	
HIF-1-alpha transcription factor network	3.70E-17
ATF-2 transcription factor network	3.00E-03
AP-1 transcription factor network	5.20E-03
Validated transcriptional targets of deltaNp63 isoforms	2.10E-02
IL6-mediated signaling events	2.10E-02
<b>Group 5 DR</b>	
E2F transcription factor network	3.00E-09
Fanconi anemia pathway	7.40E-08
ATM pathway	1.20E-05

Table 4: Enriched GSEA terms of DEGs. Canonical pathways associated with up- (UR) and down- regulated (DR) genes in groups 2, 3, 4, and 5, in comparison to group 1.

On the other hand, downregulated genes in group 4 are involved in glucocorticoid receptor regulatory network (Table 4). When comparing the profile of proposed model (group 5) to that of conventional HepG2 culture (group 1), co-culturing HepG2 spheroids with SV-80 cells grown in 3D culture upregulated genes involved in Src-homology 2 domain-containing phosphatase 2 (SHP2) signaling in addition to HIF1 $\alpha$ , AP-1, IL-6, ATF-2 networks. Moreover, upregulated genes in group 5 are transcriptional targets of deltaNp63 (Table 4). Downregulated genes are involved in E2F, Fanconi anemia, and Ataxia telangiectasia-mutated (ATM) (Table 4).

To assess the enriched GO terms in respect to biological processes, all significant DEGs of different culturing conditions were analyzed using BiNGO. Relevant GO terms are shown in Table 5. Upregulated genes in all groups (in comparison to group 1) were enriched in GO terms related to response to hypoxia, even in CoCl<sub>2</sub> non-treated 3D culture groups, indicating the formation of hypoxic core in 3D culture spheroids. In addition, upregulated genes of all groups were enriched in GO terms related to response to endogenous stimulus. However, only groups co-cultured with fibroblasts (group 3 and 5) were enriched in GO terms related to response to external stimulus, in other words, response to an environmental stimulus outside the cancer cell (Table 5). Group 5 upregulated genes set was especially enriched in GO terms related to tissue, organ, and vasculature developments. Moreover, enriched GO terms included multicellular organismal development (Figure 10). Using Venn diagram, overlapping genes between development terms were identified. For instance, 21 genes overlapped between all development terms (Figure 11a). Expression of genes involved in was compared among all culturing conditions using a heatmap to explore how different groups express this set of genes (Figure 11b). As expected, group 5 exhibited an overall

upregulation of these genes, resulting in clustering separately from the rest of the groups. Interestingly, the two other clusters formed between groups 1 and 3, and groups 2 and 4, based on their expression of multicellular organismal development-related genes.

<b>Upregulated Group 2</b>		
<b>Term</b>	<b># Genes</b>	<b>FDR</b>
response to chemical stimulus	47	0.0000002
response to hypoxia	11	0.0002930
negative regulation of programmed cell death	16	0.0013031
response to endogenous stimulus	17	0.0040785
<b>Upregulated Group 3</b>		
<b>Term</b>	<b># Genes</b>	<b>FDR</b>
response to wounding	36	0.0000042
response to endogenous stimulus	35	0.0000016
negative regulation of apoptosis	24	0.0005909
response to external stimulus	31	0.0003799
response to hypoxia	20	0.0000002
<b>Upregulated Group 4</b>		
<b>Term</b>	<b># Genes</b>	<b>FDR</b>
response to endogenous stimulus	15	0.0088056
wound healing	10	0.0038006
extracellular matrix organization	6	0.0214460
response to hypoxia	7	0.0275870
<b>Upregulated Group 5</b>		
<b>Term</b>	<b># Genes</b>	<b>FDR</b>
tissue development	75	0.0011047
vasculature development	39	0.0000743
organ development	156	0.0003272
multicellular organismal development	236	0.0006308
response to hypoxia	33	0.00000004
response to external stimulus	62	0.0002584
response to endogenous stimulus	60	0.0000373
negative regulation of apoptosis	52	0.0000070

Table 5. Enriched GO terms associated with upregulated genes. Biological processes of upregulated genes in groups 2, 3, 4, and 5.

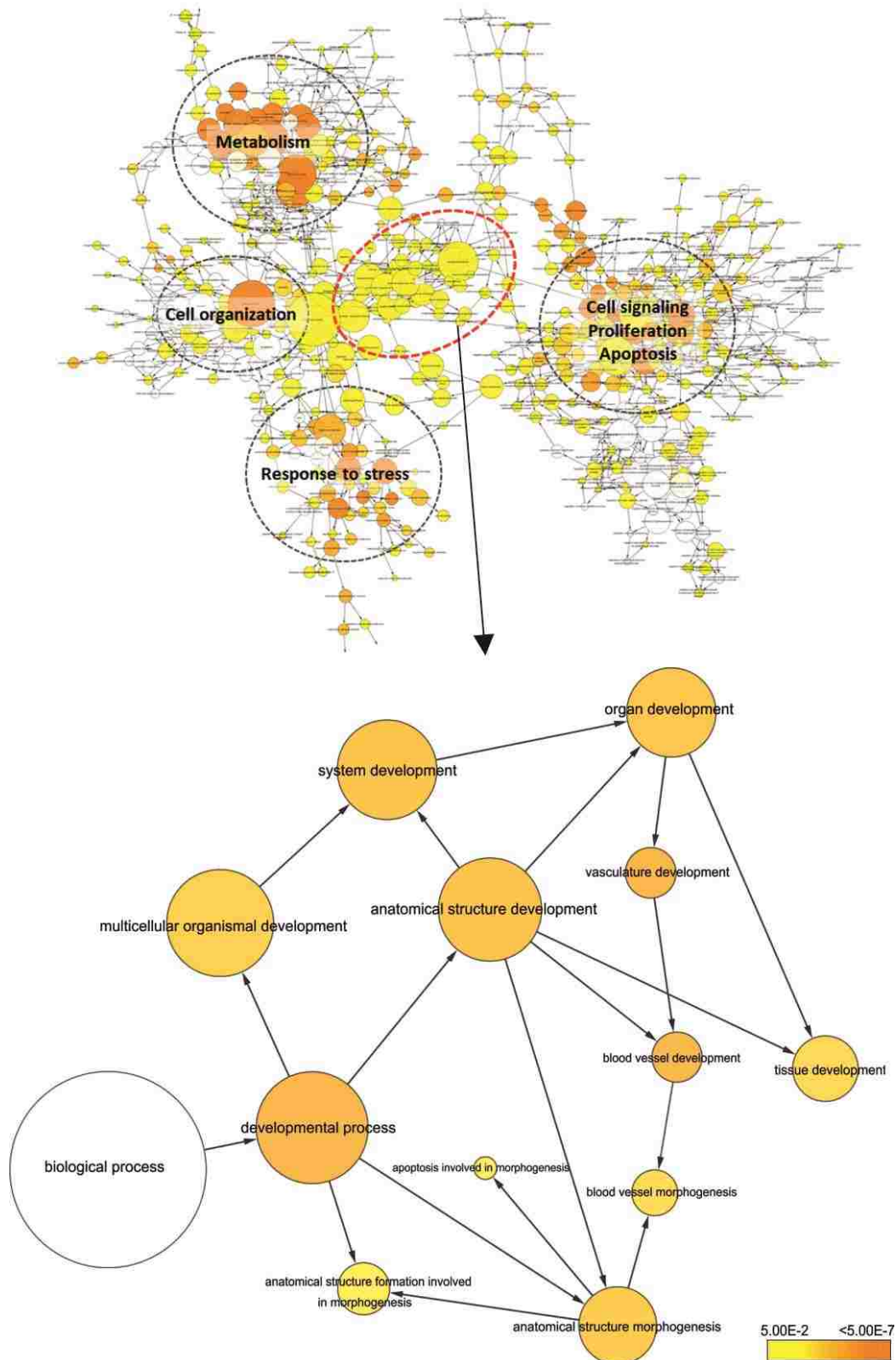


Figure 10: Network of GO categories of upregulated genes in group 5. GO term overrepresentation of up-regulated genes of group 5. The size of each node reflects the number of genes and the color indicates different levels of significance for the enriched terms according to the included key.

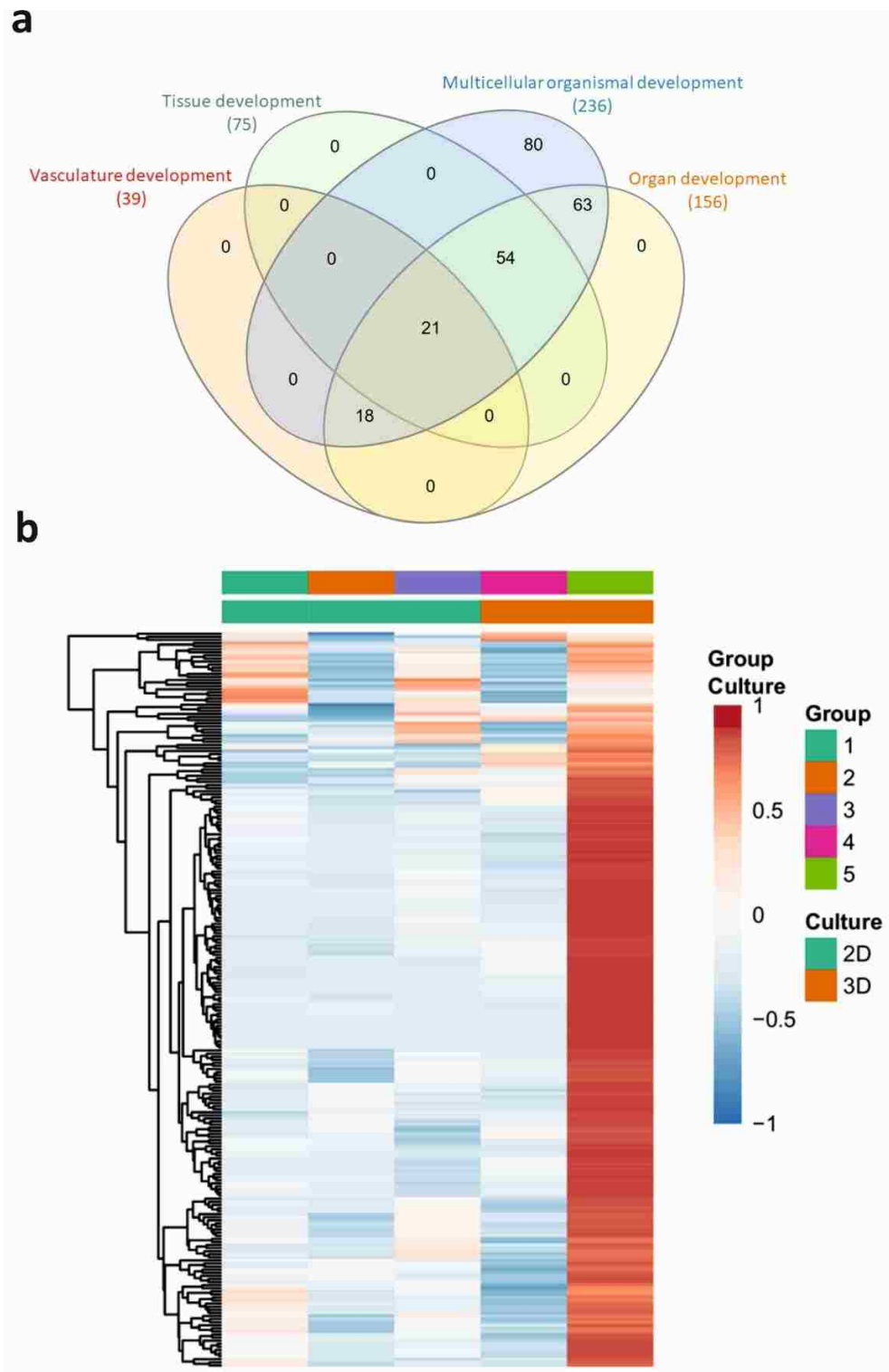


Figure 11: Venn diagram and heatmap for genes of GO terms of interest. a) Venn diagram of genes associated with tissue, organ, vasculature, and multicellular organismal developments in group 5. b) Heatmap of expression of genes associated with and multicellular organismal development in all groups. Triplicates of each group are collapsed by taking mean inside each group. Rows are centered; vector scaling is applied to rows. Rows are clustered using Euclidean distance and average linkage. 238 rows, 5 columns.

GO terms associated with the downregulated genes sets were also obtained from BiNGO. Group 3 downregulated genes set turned out only two enriched GO terms; negative regulation of transcription and negative regulation of RNA metabolic process, both of which were common with group 2. In addition, group 2 downregulated gene set was enriched in GO terms related to negative regulation of gene expression. On the other hand, certain GO terms overlapped between group 4 and 5, where downregulated genes were enriched in terms related to cell cycle regulation. Other enriched terms were attributed to culturing HepG2 under 3D conditions, such as negative regulation of cell adhesion and regulation of microtubule cytoskeleton organization (Table 6).

<b>Downregulated Group 2</b>		
<b>Term</b>	<b># Genes</b>	<b>FDR</b>
negative regulation of cellular metabolic process	10	0.0414870
negative regulation of RNA metabolic process	9	0.0079778
negative regulation of transcription	9	0.0123420
<b>Downregulated Group 3</b>		
<b>Term</b>	<b># Genes</b>	<b>FDR</b>
negative regulation of transcription, DNA-dependent	11	0.0203720
negative regulation of RNA metabolic process	11	0.0203720
<b>Downregulated Group 4</b>		
<b>Term</b>	<b># Genes</b>	<b>FDR</b>
cell cycle arrest	4	0.0191050
regulation of cell proliferation	12	0.0087652
negative regulation of cell adhesion	4	0.0040171
regulation of cell-substrate adhesion	4	0.0053097
<b>Downregulated Group 5</b>		
<b>Term</b>	<b># Genes</b>	<b>FDR</b>
response to DNA damage stimulus	54	0.000000000001
cell cycle checkpoint	21	0.0000002
DNA damage checkpoint	13	0.0000305
regulation of microtubule cytoskeleton organization	7	0.0375770

Table 6: Enriched GO terms associated with downregulated genes. Biological processes of downregulated genes in groups 2, 3, 4, and 5.



### 3.7 PPI Networks

Genes associated with multicellular organismal development mapped using Network Analyst to construct PPI networks, generating a network of 1968 nodes and 3941 edges (Figure 12 a). To identify key regulators in the constructed network, module detection was performed using Module Explorer function on Network Analyst. The top identified modules were then mapped onto the network to visualize their PPI pattern (Figure 12 b). The regulators of the top modules were JUN, epidermal growth factor receptor (EGFR), and histone deacetylase 3 (HDAC3).

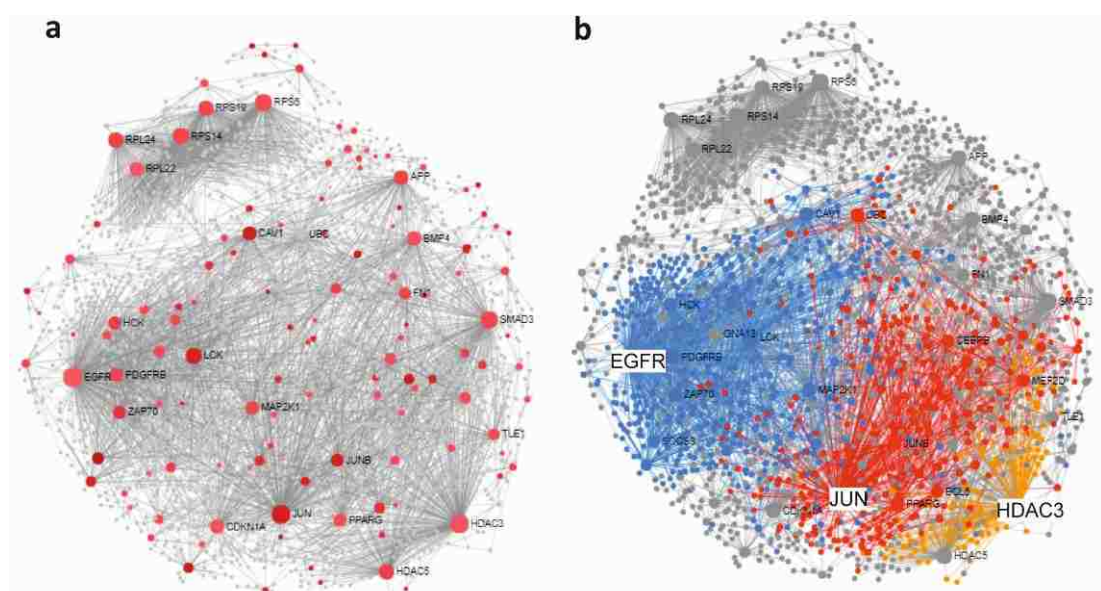


Figure 12: PPI network of multicellular organismal development. a) PPI network were generated based on the list of genes associated with multicellular organismal development and their corresponding fold change in group 5. Upregulated genes are indicated in red, where darker shade corresponds to higher expression. b) Key regulators of genes driving multicellular organismal development were identified as EGFR (blue), HDAC3 (orange), and JUN (Red).

Nodes under the regulation of the aforementioned regulators (Figure 12 b) were extracted and subjected to GO enrichment analysis. HDAC3-regulated module was enriched in terms related to chromatin organization, regulation of gene expression, and cellular component organization. JUN-regulated module was enriched in terms related

to regulation of gene expression, multicellular organismal development, organ development, and liver development. EGFR-regulated module GO terms were mostly enriched in signaling pathways and cell communication, but they were also enriched in terms related to organ development, tissue development, and multicellular organismal development (Table 7).

Term	# Genes	FDR
<b>HDAC3</b>		
chromatin organization	56	2.18E-51
regulation of gene expression	87	1.85E-32
cellular component organization	69	1.02E-20
<b>JUN</b>		
regulation of gene expression	226	5.75E-89
organ development	122	1.13E-32
multicellular organismal development	151	8.03E-28
liver development	12	8.94E-08
<b>EGFR</b>		
signaling	321	0.00E+00
signal transduction	232	1.80E-80
regulation of cell communication	162	1.82E-59
organ development	166	2.13E-36
multicellular organismal development	199	3.49E-25
tissue development	70	3.40E-14

Table 7: Enriched GO terms associated with key regulators in group 5. Biological processes of genes within modules regulated by HDAC3, JUN, and EGFR.

### 3.8 Validation by qPCR

To validate both RNA-Seq data and certain genes of interest in group 5, qPCR was carried out, in triplicates. When plotting log fold change from both experiments together, the two datasets superimpose on each other in most genes, with few exceptions. Nonetheless, non-superimposed datasets did show similar expression trends, reflecting expression levels observed in RNA-Seq data (Figure 13).

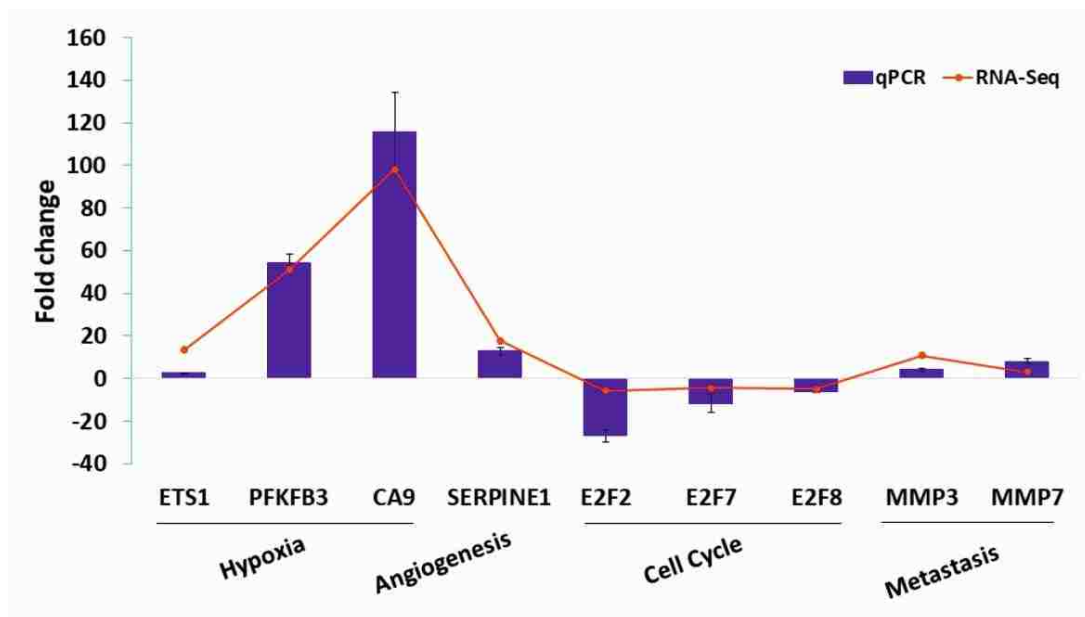


Figure 13: Validation by qPCR. RNA-Seq based expression was plotted against qPCR-based expression. qPCR data are represented as means of fold change  $\pm$  SD.

## Chapter 4: Discussion

Cancer is characterized by chaotically and rapidly dividing cells spinning out of control. The cell-centered view that reduces cancer to isolated cancer cells distorts our understanding of the multifactorial malignant process. For the seed to grow, a suitable soil must be provided; as such, an encouraging microenvironment plays a key role in driving tumor progression (Hanahan and Weinberg, 2011; Konopleva and Jordan, 2011; Balkwil et al., 2012; Hanahan and Coussens, 2012; Quail and Joyce, 2013; Klemm and Joyce, 2015).

The study presented in this thesis investigated how architecture and context of the cell contribute to tumorigenesis. To address this notion, liver cancer microenvironment was modeled using a 3D co-culture system that included both liver cancer cells and non-malignant stromal cells (fibroblasts). This model was, then, compared to other culturing methods in terms of their transcriptome profiles to reveal significant differences, if any, leading to a more aggressive phenotype.

As shown in Figures 6 and 7, morphology of HepG2 and SV-80 cells grown in 3D culture was highly distinct from their 2D counterparts. Distribution of 2D culture was restricted to the surface of the culturing substrate, limiting cell-cell communication to the perimeter of the cell. This limitation was eliminated in 3D cultures, where cells could spread in all three dimensions and to be layered on top of each other, thus, creating an oxygen, nutrient and waste gradients (Mehta et al., 2012). 3D culture has been reported to alter cellular morphology, resulting in enhanced cell-cell communication and response to stimuli (Anton et al., 2015).

In this study, the transcriptome of five culturing conditions was profiled to determine the effects of each condition on tumorigenesis. PCA and hierarchical cluster

heatmap were performed on all groups to estimate how similar/ different the groups are, based on their gene expression profile. In a PCA plot, the distance between any two points is correlated to their similarity; in other words, the closer two points are, the more similar they are, and vice versa. As shown in Figure 9 a, group 5 was on one extreme of all the other groups, specifically group 1, which was the furthest point on the plot from group 5. This clear distinction suggests a fundamental difference in gene expression between the proposed model and all other culturing conditions. Consistently, the hierarchical cluster heatmap shown in Figure 9 b revealed a similar distribution, where group 5 clustered separately from the rest of the groups. Interestingly, HepG2 cells grown in 2D co-culture (group 3) clustered with 3D HepG2 spheroids (group 4) and not with the other 2D culture groups (group 1 & 2); suggesting a considerable change in gene expression as a result of co-culture with fibroblasts.

#### **4.1 Effects of Hypoxia Mimicking-conditions**

By increasing the layers of complexity in each group, DEGs associated with each element of complexity were identified. For instance, by only culturing HepG2 cells under hypoxia-mimicking conditions (group 2), a set of genes that act as direct effectors of p53 were upregulated. In addition, mimicked hypoxia resulted in upregulating transcriptional targets of  $\Delta$ Np63, and AP-1 transcription network (Table 4). P53 gene family includes p53, p63, and p73; all of which work as transcription factors regulating key pathways such as cell proliferation, apoptosis, development, and differentiation (Inoue and Fry, 2014). Splice variants of p63 and p73 that include the N-terminal transactivation domain (TA) homologous to that of p53 are referred to as TAp63 and TAp73, respectively. These splice variants act as tumor suppressors *in vivo* mouse models (Guo et al., 2009; Tomasini et al., 2008). However, splice variants of

p63 and p73 that do not include the TA domain are referred to as  $\Delta N$  (amino-truncated) isoforms  $\Delta Np63$  and  $\Delta Np73$  (Kaghad et al., 1997; Yang et al., 1998). These truncated variants act as oncogenes by antagonizing p53, TAp63, and TAp73 through competitive binding to target DNA-binding sites and/ or through the formation of complexes with TAp63, TAp73, and p53 (Yang et al., 1998; Davison et al., 1999; Chi et al., 1999; Grob et al., 2001; Stiewe et al., 2002; Chan et al., 2004). AP-1 proteins (*i.e.* Jun, Fos, and Atf families) are involved in a number of cellular processes, including proliferation and apoptosis through the modulation of cell cycle regulators such as p53 family. AP-1 proteins are activated by hypoxia and are frequently deregulated in cancer, indicating their pro-cancer role (Angel and Karin, 1991; Eferl and Wagner, 2003; Vlahopoulos et al., 2008).

As revealed by GSEA, culturing HepG2 cells under hypoxia-mimicking conditions resulted in upregulation of AP-1 and ATF-2 transcription factor networks, and the transcriptional targets of  $\Delta Np63$ ; suggesting an antagonizing effect on p53. Such observations are reflected in GO enrichment analysis, where upregulated genes were enriched in terms related to negative regulation of programmed cell death, suggesting an inhibition of apoptosis in HepG2 cells grown under hypoxia-mimicking conditions. GSEA of downregulated genes in group 2 revealed that enriched terms were related to “genes encoding secreted soluble factors” and “genes encoding ECM-associated proteins including ECM-affiliated proteins, ECM regulators and secreted factors”. Surprisingly, the subset of genes associated with this term are involved in migration and invasion.  $CoCl_2$  treatment only resulted in inhibiting apoptosis, which is consistent with previous reports (Piret et al., 2002; Piret et al., 2004); however, it did not encourage other cancer promoting hallmarks, such as invasion. GO enrichment analysis of downregulated genes revealed that culturing HepG2 cells under hypoxia-

mimicking conditions decreased negative regulation of transcription, which could be attributed to the increase in transcription of HIF pathway target genes needed for survival under hypoxia (Liu and Simon, 2004).

#### **4.2 Effects of Stromal Signaling in 2D Microenvironment Model**

To examine the role of the stroma in cancer progression, group 3 and 5 were developed. In group 3, a simple one-way communication culturing system was established by incubating HepG2 cells with the conditioned media of SV-80 cells. In addition, HepG2 cells were treated with CoCl<sub>2</sub> to mimic hypoxic conditions. As a result, HepG2 cells transcriptome profile indicated that group 3 culturing conditions promote a tumor-supporting gene expression. Interestingly, the one-way communication system upregulated genes associated with integrin cell surface interactions, in addition to uPA and uPAR-mediated signaling. Integrins are transmembrane receptors, and they comprise the majority of cell surface receptors related to cell adhesion (Hynes, 2002). As bidirectional transmembrane receptors, integrin signaling pathway regulates many cellular processes (i.e. proliferation, survival, migration, gene expression, and ECM remodeling) within the cell in response to extracellular stimulus. It also regulates the interaction with the extracellular environment in response to intracellular cues (Hynes, 2002; Ridley et al., 2003; Schwartz and Ginsberg, 2002; Askari et al., 2009). Expectedly, integrin signaling pathway is hijacked and augmented by cancer cells to promote their own survival, invasiveness, and proliferation (Hamidi et al., 2016).

Indeed,  $\beta$ 1 integrins are overexpressed in many tumors, and blocking their signaling transduction reduces survival and tumorigenicity of many cancers, in 2D and 3D *in vitro* cultures, and *in vivo* (Paulus et al., 1993; Barkan and Chambers, 2011;

Fabricius et al., 2011; Lahlou and Muller, 2011; Schaffner et al., 2013; Vallo et al., 2017; Yang et al., 2003; Grzesiak and Bouvet, 2007; Park et al., 2006; White et al., 2004). Integrin signaling pathway transduction has been reported to be promoted by other cell surface proteins, such as urokinase receptor (uPAR) (Kugler et al., 2003). Suppressing uPAR expression or disruption uPA/uPAR interaction have been reported to inhibit tumor progression and metastasis (Lakka et al., 2001; Rao, 2005; Tyndall et al., 2008).

GO enrichment analysis yielded comparable results, where the top enriched terms associated with upregulated genes of group 3 are related to responses to endogenous and external stimuli. In addition, GSEA terms associated with upregulated genes include IL-6 mediated signaling. This is consistent with Integrin increased signaling, where enhanced IL-6/ STAT3 signaling is promoted by  $\beta$ 1-Integrin pathway (Shain et al., 2009; Kesanakurti et al., 2013). IL-6 is essential for liver regeneration, however, IL-6 persistent expression and its downstream targets have been implicated in HCC development (Schmidt-Arras and Rose-John, 2016).

Similarly, down-regulated genes in group 3 were associated with a more aggressive phenotype. GSEA terms of downregulated genes in group 3 are associated with Wnt-mediated signal transduction, including DKK1 and DKK4, inhibitors of Wnt signaling pathway. DKK1 overexpression has been reported to inhibit proliferation and invasion of gastric cancer, *in vitro* and *in vivo* (Jia et al., 2016). Overexpression of DKK1 significantly reduced tumor growth in melanoma-xenograft model, in addition to inhibiting angiogenesis (Park et al., 2014). Indeed, DKK-1 expression was found to be downregulated or lost in nine different human melanoma cell lines and most of the tested melanoma tissue samples (Kuphal et al., 2006). Similarly, Eight HCC cell lines



and 47% of 81 tissue samples were reported to express lower levels of DKK4, in comparison to their non-malignant counterparts (Fatima et al., 2012). Overexpressing DKK4 in HCC cell lines was shown to inhibit their proliferation, colony formation, and migration. In addition, xenograft models established with DKK4-expressing HCC cells exhibited a smaller tumor size (Fatima et al., 2012). GO enrichment analysis of downregulated genes in group 3 only yielded two terms, negative regulation of transcription and negative regulation of RNA metabolic process; much similar to downregulated genes in group 2. These findings demonstrate the role of stroma in supporting the malignant process through promoting tumor progression and pro-survival signaling pathways.

### **4.3 Effects of Spatial Arrangement in 3D Culture**

To explore the changes in gene expression in response to 3D culture, HepG2 spheroids were developed using poly-Hema coated culture plates. Without treatment with  $\text{CoCl}_2$ , HepG2 spheroids upregulated genes were associated with HIF1- $\alpha$  and HIF2- $\alpha$ , as revealed by GSEA. This is consistent with the body of literature promoting cancer spheroids as candidate solid tumor model, as they recapitulate many aspects of *in vivo* tumors including hypoxia (Kimlin et al.; 2013). Hypoxia development results in inducing hypoxia-mediated pathways such as HIF pathway to promote survival, angiogenesis, invasion, and metastasis (Luo et al., 2014). Indeed, silencing of both HIF1- $\alpha$  and HIF2- $\alpha$  resulted in inhibiting growth of HepG2 spheroids. However, knocking down one of them enhanced the expression of the other, increasing spheroid size and favoring survival pathways (Menrad et al., 2010). HIF1- $\alpha$  has been implicated in many aspects of liver cancer progression including epithelial–mesenchymal transition (EMT). HIF1- $\alpha$  mediated EMT has been reported to involve Wnt/  $\beta$ -catenin

signaling pathway, through hypoxia-induced overexpression of  $\beta$ -catenin (Liu et al., 2010), which in turn forms a complex with HIF1- $\alpha$ , amplifying its transcriptional activity (Zhang et al., 2013).

GSEA also identified a subset of upregulated genes in group 4 as genes encoding ECM and ECM-associated proteins, and genes encoding enzymes and their regulators involved in ECM remodeling. Abnormal ECM deposition and degradation are part of ECM remodeling, a common hallmark of hypoxia, through which it enhances cancer progression (Petrova et al., 2018). Both EMT and ECM remodeling are instrumental in the metastatic process, where ECM remodeling and degradation paves the way for migrating cancer cells to invade other locations (Rajesh and Mandal, 2017). Similarly, GO enrichment analysis of upregulated genes revealed that enriched terms are related to ECM organization and wound healing.

Similarly, GSEA of downregulated genes of group 4 revealed one term within the cutoff threshold, which is “glucocorticoid receptor regulatory network”. Glucocorticoids (GC) and their receptors (GCR) play a vital role in maintaining homeostasis of the liver under metabolic and physiological stress (Mueller et al., 2012). Indeed, GC-GCR signaling have been implicated in protecting the liver from fatty liver disease and HCC development. In GCR knockout mice, a subset of the animals developed dysplastic nodules; however, most animals developed HCC, accompanied by increased Reactive oxygen species (ROS) level and liver damage markers (Mueller et al., 2011). GO enrichment analysis revealed that downregulated genes in group 4 were enriched in terms related to negative regulation of cell adhesion. This is consistent with the proposed notion of EMT induction in response to HIF pathways and ECM remodeling observed in the upregulated genes set. In addition,

downregulated genes were enriched in terms related to cell cycle arrest and regulation of cell proliferation, indicating deregulation in cell cycle checkpoints. Taken together, these results demonstrate how upgrading HepG2 cells from 2D to 3D culture introduces hypoxia and its associated hallmarks, which better represents *in vivo* conditions.

#### **4.4 Modeling the Microenvironment of Liver Cancer**

In the aim of recapitulating the complex liver cancer TME, an *in vitro* model was developed based on a 3D co-culture system of liver cancer cells and stromal fibroblasts. Like group 4, HepG2 spheroids of the proposed model (group 5) upregulated genes were associated with HIF pathways, without being treated with  $\text{CoCl}_2$ . In addition, group 5 shared a number of enriched terms with  $\text{CoCl}_2$ - treated groups (group 2 and 3). For instance, terms related to AP-1 and ATF-2 transcription factors networks overlapped between group 2, 3, and 5. As part of AP-1 family, ATF-2 plays a role in regulating apoptosis, drug resistance, and cell cycle progression (Bhoumik et al., 2007). Deregulation of ATF-2 and its network have been implicated in liver development, regeneration, and cirrhosis (Breitwieser et al., 2007; Behnke et al., 2012). In addition, ATF-2 has been reported to play a role in HCC resistance to sorafenib, *in vivo* (Rudalska et al., 2014). This is consistent with other reports implicating AP-1 network member, c-Jun, with sorafenib resistance (Chen et al., 2016; Haga et al., 2017). Such observations are in line with hypoxia activation of AP-1 and with findings indicating that highly hypoxic HCC are resistant to sorafenib (Liang et al., 2013).

Group 5 upregulated genes also shared “IL-6 mediated signaling events” term with group 3. IL-6 overexpression has been reported in many cancers, including HCC,

where it is suggested to play a role in epithelia-stroma communication. IL-6 was reported to promote the transition of fibroblasts to CAFs (Lee et al., 2015; Yeh et al., 2015). After which, transformed CAFs overexpress and secrete IL-6 to promote growth, migration, and EMT of the cancer cells (Li et al., 2015). Indeed, studies on different types of cancer, including those of the gastrointestinal tract, have identified CAFs as the main source of IL-6, promoting tumorigenesis. For instance, CAFs in colorectal cancer microenvironment were reported to overproduce IL-6 leading to propagation of colorectal cancer cells with stem-like properties (Huynh et al., 2016). In gastric cancer, a similar overproduction of IL-6 was attributed to CAFs, where they promoted tumorigenesis through activation of Signal transducer and activator of transcription 3 (STAT3), which in turn promotes cell survival migration/ invasion and angiogenesis (Kinoshita et al., 2013; Kanda et al., 2004; Okamoto et al., 2011; Gong et al., 2005). Similarly, proliferation, migration, and invasion of liver cancer cells were enhanced by CAFs upregulation of IL-6, among other cytokines (Lin et al., 2012). These findings are consistent with GSEA, where IL-6 mediated signaling was only identified in co-culture groups, group 3 and 5, accompanied by upregulation of IL-6 receptor.

According to GSEA, downregulated genes were associated with E2F transcription factor network, Fanconi anemia pathway, and ATM pathway. ATM and BRCA1 genes were shared among the three pathways associated genes lists. ATM plays a strategic role in preserving genomic integrity through triggering cell cycle checkpoints. Hence, downregulation of ATM signaling pathway has been reported to result in chemoresistance in several cancers through impairing DNA damage response, bypassing cell cycle checkpoints, and therefore, harboring genomic instability (Song et al., 2007; Jiang et al., 2009; Wang et al., 2012; Rondeau et al., 2015; Yao et al.,

2017). Similarly, BRCA1 is involved in maintenance of genomic stability, DNA damage repair, and cell checkpoint control. As a tumor suppressor, BRCA1 mutations increase the risk of cancers other than breast and ovarian cancers, including stomach, liver, pancreatic, prostate, and colorectal cancers (Moran et al., 2012; Iqbal et al., 2012; Phelan et al., 2014). BRCA1 and BRCA2 have been reported to interact with Fanconi anemia family to promote DNA repair (Garcia-Higuera et al., 2001; D'Andrea and Grompe, 2003). Fanconi anemia proteins are activated in response to DNA damage, where they recruit DNA repair proteins, and activate cell cycle checkpoints (Kennedy and D'Andrea, 2005). Consistently, E2F transcription factor network, which was associated with down regulated genes of group 5, are involved in cell cycle regulation and DNA damage response. Levels of E2F1 and E2F2 have been reported to increase under DNA damage in E2F3-dependent manner, where E2F3 activity is needed for DNA damage-induced apoptosis (Martinez et al., 2010). Similarly, E2F7 and E2F8 are induced in response to DNA damage, and their downregulation prevents cell cycle arrest (Zalmas et al., 2008; Thurlings et al., 2017). In addition, inhibition of E2F7 has been reported to improve cell cycle re-entry and clonogenic survival (Mitxelena et al., 2018). GSEA of downregulated genes indicating escape of cell cycle checkpoints was well reflected in GO enrichment analysis yielded terms. Downregulated genes of group 5 were enriched in terms related to response to DNA damage stimulus, cell cycle checkpoint, and DNA damage checkpoint.

GO enrichment analysis of upregulated genes yielded very interesting results. Group 5 enriched terms were related to response to external stimulus. Group 5, in addition to group 3, were the only groups enriched in terms related to response to external stimulus, highlighting the interaction with fibroblasts in the co-culture models. In addition, Group 5 enriched terms were related to vasculature development,

tissue development, organ development, and multicellular organismal development. As shown in Figure 11 a, 21 genes were shared among the four terms, 63 genes were associated with both organ development and multicellular organismal development, whereas 80 genes were unique to multicellular organismal development, indicating non-redundancy in identifying these GO terms. Heatmap visualization of genes associated with multicellular organismal development revealed a specific upregulation of these genes in group 5 in comparison to all other groups.

Through PPI networks, modules associated with multicellular organismal development were identified. Modules could be defined as clusters within a network that carry a number of connections that cannot be, otherwise, formed randomly. Regulators of modules associated with multicellular organismal development were identified to be JUN, EGFR, and HDAC3. Genes under the regulation of JUN were enriched in terms related to development of organ and liver, and multicellular organismal development. As mentioned earlier, JUN is involved in the regulation of survival, proliferation, and apoptosis. JUN is upregulated in many cancers, including HCC, where it has been shown to play a role in liver development, regeneration, and induction of liver cancer through inhibition of apoptosis (Stepniak et al., 2006; Eferl et al., 2003). EGFR activation has been reported to be partially regulated by JUN, where inhibition of c-Jun (protein encoded by JUN) led to a significant suppression of EGFR transcription in bladder cancer cells. In addition, higher expression of EGFR was correlated with enhanced metastasis, *in vitro* and *in vivo* (Fang et al., 2014). Genes under the regulation of EGFR were enriched in terms related to cell signaling and communication, in addition to development of organ and tissue, and multicellular organismal development. Indeed, EGFR has been implicated in liver proliferation, regeneration, fibrogenesis, and neoplasticity; where it is often found to be

overexpressed (Komposch and Sibilina, 2016; Berasain and Avila, 2014). EGFR signaling pathway cross-talks with many other signaling pathways regulating development and progression of HCC, highlighting it as a signaling hub (Berasain et al., 2011). Both JUN and EGFR have been reported to be affected by HDAC3 expression, where inhibition of HDAC3 resulted in suppressing the expression of c-Jun and EGFR (Yamaguchi et al., 2005; Chou et al., 2011). HDAC3, as a member of the HDAC family, is involved in regulation of gene transcription. HDAC3 is also heavily involved in liver processes, it has been reported to play an important role in liver regeneration and proliferation (Lu et al., 2018). As such, HDAC3 was reported to be a specific requirement for liver formation in zebrafish, where inhibiting HDACs led to hindering liver development (Farooq et al., 2008). HDAC3 is found to be overexpressed in many cancers, including liver cancer, where inhibition of HDAC3 resulted in repressed cancer growth *in vitro*, and inhibition of tumor growth *in vivo* (Lu et al., 2018). In addition, HDAC3 has been implicated in liver cancer stem cells self-renewal (Liu et al., 2013). Based on GO enrichment analysis of PPI network modules (Figure 12), genes under the regulation of HDAC3 were enriched in terms related to chromatin organization, regulation of gene expression, and regulation of metabolic process.

Culturing HepG2 in 3D co-culture system also modulated expression of a number of genes linked to driving HCC progression and are associated with a more aggressive phenotype. qPCR was carried out to compare the expression of genes of interest between group 1 and group 5; including CA9, PFKFB3, SERPINE1, ETS1, MMP3, MMP7, E2F2, E2F7, and E2F8. CA9 is upregulated in all groups, in comparison to group 1; however, group 5 exhibited almost 100-fold increase, which was confirmed by qPCR (Figure 13). CA9 is upregulated under hypoxia and is transcriptionally

regulated by HIF1- $\alpha$  (Wykoff et al., 2000), and therefore, can be used as a substitute marker for HIF1 transcriptional activity (Kaluz et al., 2009). Overexpression of CA9 has been reported in different cancer types, promoting survival through modulating migration, invasion, and EMT (McDonald et al., 2012; Shin et al., 2011; Hyuga et al., 2017). CA9 serves as a prognostic marker in different cancer types, including liver cancer, where expression of CA9 is a predictor of poor prognosis in cases of resectable HCC in addition to advanced HCC (Kang et al., 2015; Huang et al., 2015). Similarly, PFKFB3, is upregulated in all groups in comparison to group 1, with the highest fold change exhibited in group 5. PFKFB3 is a direct target of HIF1, where it regulates glucose metabolism and promotes cancer progression and growth (Lu et al., 2017). Overexpression of PFKFB3 is often associated with an aggressive phenotype and poor prognosis (Clem et al., 2013). Indeed, PFKFB3 expression is associated with poor prognosis of HCC, and its inhibition resulted in suppression of HCC growth *in vitro* and *in vivo* (Shi et al., 2018), in addition to rendering sorafenib-resistant HCC cell lines sensitive to treatment (Li et al., 2017).

Culturing HepG2 under 3D co-culture conditions also enhanced the expression of genes promoting angiogenesis, migration, and invasion such as SERPINE1, ETS1, MMP3, and MMP7. SERPINE1 is upregulated in all groups in comparison to group 1, with the highest fold change exhibited in group 5. Increased expression of PAI-1 (encoded by SERPINE1), is correlated with aggressive cancers and poor prognosis, where it is also associated with migration, invasion, and angiogenesis in HCC tissue (Placencio and DeClerck, 2015; Zheng et al., 2000). ETS1, MMP3, and MMP7 are only upregulated in group 5, and were not differentially expressed in groups 2, 3, and 4 in comparison to group 1. ETS1 is involved in upregulating hypoxia-target genes such as CA9, in addition to MMP3, and MMP7 (Salnikow et al., 2008; Dittmer, 2003;



Ozaki et al., 2000). Downregulation of ETS1 was reported to inhibit metastasis and invasion of liver and gastric cancer cell lines (Cao et al., 2015; Ma et al., 2015; Zheng et al., 2013). Similarly, Expression of MMP3 and MMP7 is correlated with enhanced metastatic phenotype, where their inhibition suppressed invasion and migration of HCC cells (Monvoisin et al., 2002; Lin et al., 2017; Tu et al., 2014).

Culturing HepG2 under 3D co-culture conditions also downregulated the expression of genes involved cell cycle regulation and survival, including E2F2, E2F7, and E2F8. E2F transcription factors were only differentially expressed in group 5, where they were found to be downregulated in comparison to group 1, which was confirmed by qPCR (Figure 8). As previously discussed, downregulation of E2F2, E2F7, and E2F8 prevents cell cycle arrest and enhances clonogenic survival. Taken together, these findings indicate that culturing HepG2 under conditions of group 5 result in an aggressive phenotype with enhanced migration, invasion, metastasis, and angiogenesis.

## Chapter 5: Conclusion

In the study presented herein, an *in vitro* model of liver cancer microenvironment was proposed to better mimic *in vivo* settings. By creating a setting where HepG2 spheroids were co-cultured with stromal fibroblasts, an *in vivo* context was established where liver cancer cells started expressing genes associated with liver development. In comparison to conventional 2D culture, the proposed model exhibited an increase in the expression of genes associated with development, progression, and poor prognosis of HCC. The model presented herein exhibited a gene expression profile associated with an aggressive phenotype that better mimics *in vivo* HCC, and therefore, a more reliable platform for anti-cancer drug screening.

## References

- Angel, Peter, and Michael Karin. "The Role of Jun, Fos and the AP-1 Complex in Cell-Proliferation and Transformation." *BBA - Reviews on Cancer*, vol. 1072, no. 2–3, 1991, pp. 129–57, doi:10.1016/0304-419X(91)90011-9.
- Anton, Delphine, et al. "Three-Dimensional Cell Culture: A Breakthrough in Vivo." *International Journal of Molecular Sciences*, vol. 16, no. 3, 2015, pp. 5517–27, doi:10.3390/ijms16035517.
- Askari, J. A., et al. "Linking Integrin Conformation to Function." *Journal of Cell Science*, vol. 122, no. 2, 2009, pp. 165–70, doi:10.1242/jcs.018556.
- Balkwill, F. R., et al. "The Tumor Microenvironment at a Glance." *Journal of Cell Science*, vol. 125, no. 23, 2012, pp. 5591–96, doi:10.1242/jcs.116392.
- Barkan, Dalit, and Ann F. Chambers. "β1-Integrin: A Potential Therapeutic Target in the Battle against Cancer Recurrence." *Clinical Cancer Research*, vol. 17, no. 23, 2011, pp. 7219–23, doi:10.1158/1078-0432.CCR-11-0642.
- Behnke, Martha, et al. "The Expression of Embryonic Liver Development Genes in Hepatitis c Induced Cirrhosis and Hepatocellular Carcinoma." *Cancers*, vol. 4, no. 3, 2012, pp. 945–68, doi:10.3390/cancers4030945.
- Berasain, Carmen, and Matías A. Avila. "The EGFR Signalling System in the Liver: From Hepatoprotection to Hepatocarcinogenesis." *Journal of Gastroenterology*, vol. 49, no. 1, 2014, pp. 9–23, doi:10.1007/s00535-013-0907-x.
- Berasain, Carmen, et al. "Epidermal Growth Factor Receptor (EGFR) Crosstalks in Liver Cancer." *Cancers*, vol. 3, no. 2, 2011, pp. 2444–61, doi:10.3390/cancers3022444.
- Beucken, Twan, et al. "Hypoxia-Induced Expression of Carbonic Anhydrase 9 Is Dependent on the Unfolded Protein Response." *Journal of Biological Chemistry*, vol. 284, no. 36, 2009, pp. 24204–12, doi:10.1074/jbc.M109.006510.
- Bhoulmik, Anindita, et al. "ATF2 on the Double – Activating Transcription Factor and DNA Damage Response Protein." *Pigment Cell Research*, vol. 20, no. 6, 2007, pp. 498–506, doi:10.1111/j.1600-0749.2007.00414.x.

- Bissell, Mina J., and William C. Hines. "Why Don't We Get More Cancer? A Proposed Role of the Microenvironment in Restraining Cancer Progression." *Nature Medicine*, vol. 17, no. 3, 2011, pp. 320–29, doi:10.1038/nm.2328.
- Brahimi-Horn, M.Christiane, et al. "Hypoxia and Cancer." *Journal of Molecular Medicine*, vol. 85, no. 12, 2007, pp. 1301–07, doi:10.1007/s00109-007-0281-3.
- Breitwieser, Wolfgang, et al. "Feedback Regulation of p38 Activity via ATF2 Is Essential for Survival of Embryonic Liver Cells." *Genes and Development*, vol. 21, no. 16, 2007, pp. 2069–82, doi:10.1101/gad.430207.
- Cao, Liangqi, et al. "MIR-324-5p Suppresses Hepatocellular Carcinoma Cell Invasion by Counteracting ECM Degradation through Post-Transcriptionally Downregulating ETS1 and SP1." *PLoS ONE*, vol. 10, no. 7, 2015, doi:10.1371/journal.pone.0133074.
- Casazza, A., et al. "Tumor Stroma: A Complexity Dictated by the Hypoxic Tumor Microenvironment." *Oncogene*, vol. 33, no. 14, 2014, pp. 1743–54, doi:10.1038/onc.2013.121.
- Catalano, Veronica, et al. "Tumor and Its Microenvironment: A Synergistic Interplay." *Seminars in Cancer Biology*, vol. 23, no. 6 PB, 2013, pp. 522–32, doi:10.1016/j.semcancer.2013.08.007.
- Chan, Wan Mui, et al. "How Many Mutant p53 Molecules Are Needed to Inactivate a Tetramer?" *Molecular and Cellular Biology*, vol. 24, no. 8, 2004, pp. 3536–51, doi:10.1128/MCB.24.8.3536.
- Chen, Wei, et al. "Activation of c-Jun Predicts a Poor Response to Sorafenib in Hepatocellular Carcinoma: Preliminary Clinical Evidence." *Scientific Reports*, vol. 6, 2016, doi:10.1038/srep22976.
- Chi, Seung Wook, et al. "Solution Structure of a Conserved C-Terminal Domain of p73 with Structural Homology to the SAM Domain." *EMBO Journal*, vol. 18, no. 16, 1999, pp. 4438–45, doi:10.1093/emboj/18.16.4438.
- Chou, Chia Wei, et al. "HDAC Inhibition Decreases the Expression of EGFR in Colorectal Cancer Cells." *PLoS ONE*, vol. 6, no. 3, 2011, doi:10.1371/journal.pone.0018087.
- Cirri, Paolo, and Paola Chiarugi. "Cancer-Associated-Fibroblasts and Tumour Cells: A Diabolic Liaison Driving Cancer Progression." *Cancer and*

Metastasis Reviews, vol. 31, no. 1–2, 2012, pp. 195–208, doi:10.1007/s10555-011-9340-x.

Clem, B. F., et al. “Targeting 6-Phosphofructo-2-Kinase (PFKFB3) as a Therapeutic Strategy against Cancer.” *Molecular Cancer Therapeutics*, vol. 12, no. 8, 2013, pp. 1461–70, doi:10.1158/1535-7163.MCT-13-0097.

D’Andrea, Alan D., and Markus Grompe. “The Fanconi anaemia/BRCA Pathway.” *Nature Reviews Cancer*, vol. 3, no. 1, 2003, pp. 23–34, doi:10.1038/nrc970.

Davison, Timothy S., et al. “p73 and p63 Are Homotetramers Capable of Weak Heterotypic Interactions with Each Other but Not with p53.” *Journal of Biological Chemistry*, vol. 274, no. 26, 1999, pp. 18709–14, doi:10.1074/jbc.274.26.18709.

Dittmer, Jürgen. “The Biology of the Ets1 Proto-Oncogene.” *Molecular Cancer*, vol. 2, 2003, doi:10.1186/1476-4598-2-29.

Eferl, Robert, and Erwin F. Wagner. “AP-1: A Double-Edged Sword in Tumorigenesis.” *Nature Reviews Cancer*, vol. 3, no. 11, 2003, pp. 859–68, doi:10.1038/nrc1209.

Eferl, Robert, et al. “Liver Tumor Development: C-Jun Antagonizes the Proapoptotic Activity of p53.” *Cell*, vol. 112, no. 2, 2003, pp. 181–92, doi:10.1016/S0092-8674(03)00042-4.

Fabricius, Eva Maria, et al. “Immunohistochemical Analysis of Integrins avb3, avb5 and a5b1, and Their Ligands, Fibrinogen, Fibronectin, Osteopontin and Vitronectin, in Frozen Sections of Human Oral Head and Neck Squamous Cell Carcinomas.” *Experimental and Therapeutic Medicine*, vol. 2, no. 1, 2011, pp. 9–19, doi:10.3892/etm.2010.171.

Fang, Yong, et al. “A New Tumour Suppression Mechanism by p27 Kip1 : EGFR down-Regulation Mediated by JNK/c-Jun Pathway Inhibition.” *Biochemical Journal*, vol. 463, no. 3, 2014, pp. 383–92, doi:10.1042/BJ20140103.

Farooq, Muhammad, et al. “Histone Deacetylase 3 (hdac3) Is Specifically Required for Liver Development in Zebrafish.” *Developmental Biology*, vol. 317, no. 1, 2008, pp. 336–53, doi:10.1016/j.ydbio.2008.02.034.

Fatima, S., et al. “Dickkopf 4 (DKK4) Acts on Wnt/B-Catenin Pathway by Influencing B-Catenin in Hepatocellular Carcinoma.” *Oncogene*, vol. 31, no. 38, 2012, pp. 4233–44, doi:10.1038/onc.2011.580.

- Fattovich, Giovanna, et al. "Hepatocellular Carcinoma in Cirrhosis: Incidence and Risk Factors." *Gastroenterology*, vol. 127, no. SUPPL., 2004, doi:10.1053/j.gastro.2004.09.014.
- Ferlay J. Soerjomataram I. Dikshit R., Eser S., and Ervik M. "Cancer Incidence and Mortality Worldwide: IARC CancerBase No. 11, 2013, doi:http://globocan.iarc.fr/Pages/fact\_sheets\_cancer.aspx
- Garcia-Higuera, Irene, et al. "Interaction of the Fanconi Anemia Proteins and BRCA1 in a Common Pathway." *Molecular Cell*, vol. 7, no. 2, 2001, pp. 249–62, doi:10.1016/S1097-2765(01)00173-3.
- Gilkes, Daniele M., et al. "Hypoxia and the Extracellular Matrix: Drivers of Tumour Metastasis." *Nature Reviews Cancer*, vol. 14, no. 6, 2014, pp. 430–39, doi:10.1038/nrc3726.
- Gong, W., et al. "Expression of Activated Signal Transducer and Activator of Transcription 3 Predicts Expression of Vascular Endothelial Growth Factor in and Angiogenic Phenotype of Human Gastric Cancer." *Clinical Cancer Research: An Official Journal of the American Association for Cancer Research*, vol. 11, no. 4, 2005, pp. 1386–93, doi:10.1158/1078-0432.CCR-04-0487.
- Grob, T. J., et al. "Human  $\Delta$ Np73 Regulates a Dominant Negative Feedback Loop for TAp73 and p53." *Cell Death and Differentiation*, vol. 8, no. 12, 2001, pp. 1213–23, doi:10.1038/sj.cdd.4400962.
- Grzesiak, John J., and Michael Bouvet. "Determination of the Ligand-Binding Specificities of the  $\alpha$ 2 $\beta$ 1 and  $\alpha$ 1 $\beta$ 1 Integrins in a Novel 3-Dimensional in Vitro Model of Pancreatic Cancer." *Pancreas*, vol. 34, no. 2, 2007, pp. 220–28, doi:10.1097/01.mpa.0000250129.64650.f6.
- Guo, Xuecui, et al. "TAp63 Induces Senescence and Suppresses Tumorigenesis in Vivo." *Nature Cell Biology*, vol. 11, no. 12, 2009, pp. 1451–57, doi:10.1038/ncb1988.
- Haga, Yuki, et al. "Overexpression of c-Jun Contributes to Sorafenib Resistance in Human Hepatoma Cell Lines." *PLoS ONE*, vol. 12, no. 3, 2017, doi:10.1371/journal.pone.0174153.
- Hamidi, Hellyeh, et al. "The Complexity of Integrins in Cancer and New Scopes for Therapeutic Targeting." *British Journal of Cancer*, vol. 115, no. 9, 2016, pp. 1017–23, doi:10.1038/bjc.2016.312.

- Hanahan, D., and R. A. Weinberg. "The Hallmarks of Cancer." *Cell*, vol. 100, no. 1, 2000, pp. 57–70, doi:10.1007/s00262-010-0968-0.
- Hanahan, Douglas, and Lisa M. Coussens. "Accessories to the Crime: Functions of Cells Recruited to the Tumor Microenvironment." *Cancer Cell*, vol. 21, no. 3, 2012, pp. 309–22, doi:10.1016/j.ccr.2012.02.022.
- Hanahan, Douglas, and Robert A. Weinberg. "Hallmarks of Cancer: The next Generation." *Cell*, vol. 144, no. 5, 2011, pp. 646–74, doi:10.1016/j.cell.2011.02.013.
- Heberle, Henry, et al. "InteractiVenn: A Web-Based Tool for the Analysis of Sets through Venn Diagrams." *BMC Bioinformatics*, vol. 16, no. 1, 2015, doi:10.1186/s12859-015-0611-3.
- Huang, Wei Ju, et al. "Expression of Hypoxic Marker Carbonic Anhydrase IX Predicts Poor Prognosis in Resectable Hepatocellular Carcinoma." *PLoS ONE*, vol. 10, no. 3, 2015, doi:10.1371/journal.pone.0119181.
- Huynh, Phuong T., et al. "CD90+ Stromal Cells Are the Major Source of IL-6, Which Supports Cancer Stem-like Cells and Inflammation in Colorectal Cancer." *International Journal of Cancer*, vol. 138, no. 8, 2016, pp. 1971–81, doi:10.1002/ijc.29939.
- Hynes, Richard O. "Integrins: Bidirectional, Allosteric Signaling Machines." *Cell*, vol. 110, no. 6, 2002, pp. 673–87, doi:10.1016/S0092-8674(02)00971-6.
- Hyuga, Satoshi, et al. "Expression of Carbonic Anhydrase IX Is Associated with Poor Prognosis through Regulation of the Epithelial-Mesenchymal Transition in Hepatocellular Carcinoma." *International Journal of Oncology*, vol. 51, no. 4, 2017, pp. 1179–90, doi:10.3892/ijo.2017.4098.
- Ingram, M., et al. "Three-Dimensional Growth Patterns of Various Human Tumor Cell Lines in Simulated Microgravity of a NASA Bioreactor." *In Vitro Cellular & Developmental Biology - Animal*, vol. 33, no. 6, 1997, pp. 459–66, doi:10.1007/s11626-997-0064-8.
- Inoue, Kazushi, and Elizabeth A. Fry. "Alterations of p63 and p73 in Human Cancers." *Sub-Cellular Biochemistry*, vol. 85, 2014, pp. 17–40, doi:10.1007/978-94-017-9211-0\_2.
- Iqbal, J., et al. "The Incidence of Pancreatic Cancer in BRCA1 and BRCA2 Mutation Carriers." *British Journal of Cancer*, vol. 107, no. 12, 2012, pp. 2005–09, doi:10.1038/bjc.2012.483.

- Jia, Xiaoting, et al. "miR-493 Mediated DKK1 down-Regulation Confers Proliferation, Invasion and Chemo-Resistance in Gastric Cancer Cells." *Oncotarget*, vol. 7, no. 6, 2016, pp. 7044–54, doi:10.18632/oncotarget.6951.
- Jiang, Hai, et al. "The Combined Status of ATM and p53 Link Tumor Development with Therapeutic Response." *Genes and Development*, vol. 23, no. 16, 2009, pp. 1895–909, doi:10.1101/gad.1815309.
- Kaghad, M., et al. "Monoallelically Expressed Gene Related to p53 at 1p36, a Region Frequently Deleted in Neuroblastoma and Other Human Cancers." *Cell*, vol. 90, no. 4, 1997, pp. 809–19, doi:10.1016/S0092-8674(00)80540-1.
- Kalluri, Raghu, and Michael Zeisberg. "Fibroblasts in Cancer." *Nature Reviews Cancer*, vol. 6, no. 5, 2006, pp. 392–401, doi:10.1038/nrc1877.
- Kaluz, Stefan, et al. "Transcriptional Control of the Tumor- and Hypoxia-Marker Carbonic Anhydrase 9: A One Transcription Factor (HIF-1) Show?" *Biochimica et Biophysica Acta - Reviews on Cancer*, vol. 1795, no. 2, 2009, pp. 162–72, doi:10.1016/j.bbcan.2009.01.001.
- Kanda, Naoki, et al. "STAT3 Is Constitutively Activated and Supports Cell Survival in Association with Survivin Expression in Gastric Cancer Cells." *Oncogene*, vol. 23, no. 28, 2004, pp. 4921–29, doi:10.1038/sj.onc.1207606.
- Kang, Hyo Jeong, et al. "Expression of Carbonic Anhydrase 9 Is a Novel Prognostic Marker in Resectable Hepatocellular Carcinoma." *Virchows Archiv*, vol. 466, no. 4, 2015, pp. 403–13, doi:10.1007/s00428-014-1709-0.
- Kennedy, Richard D., and Alan D. D'Andrea. "The Fanconi Anemia/BRCA Pathway: New Faces in the Crowd." *Genes and Development*, vol. 19, no. 24, 2005, pp. 2925–40, doi:10.1101/gad.1370505.
- Kesanakurti, D., et al. "Role of MMP-2 in the Regulation of IL-6/Stat3 Survival Signaling via Interaction with  $\alpha 5\beta 1$  Integrin in Glioma." *Oncogene*, vol. 32, no. 3, 2013, pp. 327–40, doi:10.1038/onc.2012.52.
- Killcoyne, Sarah, et al. "Cytoscape: A Community-Based Framework for Network Modeling." *Methods in Molecular Biology (Clifton, N.J.)*, vol. 563, 2009, pp. 219–39, doi:10.1007/978-1-60761-175-2\_12.
- Kimlin, Lauren C., et al. "In Vitro Three-Dimensional (3D) Models in Cancer Research: An Update." *Molecular Carcinogenesis*, vol. 52, no. 3, 2013, pp. 167–82, doi:10.1002/mc.21844.



- Kinoshita, Hiroto, et al. "Interleukin-6 Mediates Epithelial-Stromal Interactions and Promotes Gastric Tumorigenesis." *PLoS ONE*, vol. 8, no. 4, 2013, doi:10.1371/journal.pone.0060914.
- Klemm, Florian, and Johanna A. Joyce. "Microenvironmental Regulation of Therapeutic Response in Cancer." *Trends in Cell Biology*, vol. 25, no. 4, 2015, pp. 198–213, doi:10.1016/j.tcb.2014.11.006.
- Komposch, Karin, and Maria Sibilica. "EGFR Signaling in Liver Diseases." *International Journal of Molecular Sciences*, vol. 17, no. 1, 2016, p. 30, doi:10.3390/ijms17010030.
- Konopleva, Marina Y., and Craig T. Jordan. "Leukemia Stem Cells and Microenvironment: Biology and Therapeutic Targeting." *Journal of Clinical Oncology : Official Journal of the American Society of Clinical Oncology*, vol. 29, no. 5, 2011, pp. 591–99, doi:10.1200/JCO.2010.31.0904.
- Kugler, Matthias C., et al. "Urokinase Receptor and Integrin Interactions." *Current Pharmaceutical Design*, vol. 9, no. 19, 2003, pp. 1565–74, doi:10.2174/1381612033454658.
- Kuphal, S., et al. "Expression of Dickkopf Genes Is Strongly Reduced in Malignant Melanoma." *Oncogene*, vol. 25, no. 36, 2006, pp. 5027–36, doi:10.1038/sj.onc.1209508.
- Lahlou, Hicham, and William J. Muller. "B1-Integrins Signaling and Mammary Tumor Progression in Transgenic Mouse Models: Implications for Human Breast Cancer." *Breast Cancer Research : BCR*, vol. 13, no. 6, 2011, p. 229, doi:10.1186/bcr2905.
- Lakka, Sajani S., et al. "Adenovirus-Mediated Antisense Urokinase-Type Plasminogen Activator Receptor Gene Transfer Reduces Tumor Cell Invasion and Metastasis in Non-Small Cell Lung Cancer Cell Lines." *Clinical Cancer Research*, vol. 7, no. 4, 2001, pp. 1087–93.
- Lee, Keun Woo, et al. "Twist1 Is a Key Regulator of Cancer-Associated Fibroblasts." *Cancer Research*, vol. 75, no. 1, 2015, pp. 73–85, doi:10.1158/0008-5472.CAN-14-0350.
- Li, Pu, et al. "Epigenetic Silencing of microRNA-149 in Cancer-Associated Fibroblasts Mediates Prostaglandin E2/interleukin-6 Signaling in the Tumor Microenvironment." *Cell Research*, vol. 25, no. 5, 2015, pp. 588–603, doi:10.1038/cr.2015.51.

- Li, Sainan, et al. "By Inhibiting PFKFB3, Aspirin Overcomes Sorafenib Resistance in Hepatocellular Carcinoma." *International Journal of Cancer*, vol. 141, no. 12, 2017, pp. 2571–84, doi:10.1002/ijc.31022.
- Liang, Yingjian, et al. "Hypoxia-Mediated Sorafenib Resistance Can Be Overcome by EF24 through Von Hippel-Lindau Tumor Suppressor-Dependent HIF-1 $\alpha$  Inhibition in Hepatocellular Carcinoma." *Hepatology*, vol. 57, no. 5, 2013, pp. 1847–57, doi:10.1002/hep.26224.
- Lin, Daniel, and Jennifer Wu. "Hypoxia Inducible Factor in Hepatocellular Carcinoma: A Therapeutic Target." *World Journal of Gastroenterology*, vol. 21, no. 42, 2015, pp. 12171–78, doi:10.3748/wjg.v21.i42.12171.
- Lin, Yixiong, et al. "microRNA-489 Plays an Anti-Metastatic Role in Human Hepatocellular Carcinoma by Targeting Matrix Metalloproteinase-7." *Translational Oncology*, vol. 10, no. 2, 2017, pp. 211–20, doi:10.1016/j.tranon.2017.01.010.
- Lin, Zu Yau, et al. "Cancer-Associated Fibroblasts up-Regulate CCL2, CCL26, IL6 and LOXL2 Genes Related to Promotion of Cancer Progression in Hepatocellular Carcinoma Cells." *Biomedicine and Pharmacotherapy*, vol. 66, no. 7, 2012, pp. 525–29, doi:10.1016/j.biopha.2012.02.001.
- Liu, Chungang, et al. "Histone Deacetylase 3 Participates in Self-Renewal of Liver Cancer Stem Cells through Histone Modification." *Cancer Letters*, vol. 339, no. 1, 2013, pp. 60–69, doi:10.1016/j.canlet.2013.07.022.
- Liu, L., and M. C. Simon. "Regulation of Transcription and Translation by Hypoxia." *Cancer Biol Ther*, vol. 3, no. June, 2004, pp. 492–97, doi:1010 [pii].
- Liu, Liang, et al. "Activation of  $\beta$ -Catenin by Hypoxia in Hepatocellular Carcinoma Contributes to Enhanced Metastatic Potential and Poor Prognosis." *Clinical Cancer Research*, vol. 16, no. 10, 2010, pp. 2740–50, doi:10.1158/1078-0432.CCR-09-2610.
- Liu, Qiang, et al. "Effect of Hypoxia on Hypoxia Inducible Factor-1 $\alpha$ , Insulin-like Growth Factor I and Vascular Endothelial Growth Factor Expression in Hepatocellular Carcinoma HepG2 Cells." *Oncology Letters*, vol. 9, no. 3, 2015, pp. 1142–48, doi:10.3892/ol.2015.2879.
- Lu, Luo, et al. "The Molecular Basis of Targeting PFKFB3 as a Therapeutic Strategy against Cancer." *Oncotarget*, vol. 8, no. 37, 2017, pp. 62793–802, doi:10.18632/oncotarget.19513.

- Lu, Xu-Feng, et al. "Histone Deacetylase 3 Promotes Liver Regeneration and Liver Cancer Cells Proliferation through Signal Transducer and Activator of Transcription 3 Signaling Pathway." *Cell Death & Disease*, vol. 9, no. 3, 2018, p. 398, doi:10.1038/s41419-018-0428-x.
- Luo, Dongjun, et al. "The Role of Hypoxia Inducible Factor-1 in Hepatocellular Carcinoma." *BioMed Research International*, vol. 2014, 409272, doi:10.1155/2014/409272.
- Ma, Ning, et al. "MicroRNA-129-5p Inhibits Hepatocellular Carcinoma Cell Metastasis and Invasion via Targeting ETS1." *Biochemical and Biophysical Research Communications*, vol. 461, no. 4, 2015, pp. 618–23, doi:10.1016/j.bbrc.2015.04.075.
- Maere, Steven, et al. "BiNGO: A Cytoscape Plugin to Assess Overrepresentation of Gene Ontology Categories in Biological Networks." *Bioinformatics*, vol. 21, no. 16, 2005, pp. 3448–49, doi:10.1093/bioinformatics/bti551.
- Marsh, Timothy, et al. "Fibroblasts as Architects of Cancer Pathogenesis." *Biochimica et Biophysica Acta - Molecular Basis of Disease*, vol. 1832, no. 7, 2013, pp. 1070–78, doi:10.1016/j.bbadis.2012.10.013.
- Martinez, L. A., et al. "E2F3 Is a Mediator of DNA Damage-Induced Apoptosis." *Molecular and Cellular Biology*, vol. 30, no. 2, 2010, pp. 524–36, doi:10.1128/MCB.00938-09.
- McDonald, Paul C., et al. "Recent Developments in Targeting Carbonic Anhydrase IX for Cancer Therapeutics." *Oncotarget*, vol. 3, no. 1, 2012, pp. 84–97, doi:10.18632/oncotarget.422.
- Mehta, Geeta, et al. "Opportunities and Challenges for Use of Tumor Spheroids as Models to Test Drug Delivery and Efficacy." *J Control Release*, vol. 164, no. 2, 2012, pp. 192–204, doi:10.1016/j.jconrel.2012.04.045.
- Menrad, Heidi, et al. "Roles of Hypoxia-Inducible Factor-1alpha (HIF-1alpha) versus HIF-2alpha in the Survival of Hepatocellular Tumor Spheroids." *Hepatology (Baltimore, Md.)*, vol. 51, no. 6, 2010, pp. 2183–92, doi:10.1002/hep.23597.
- Mitxelena, Jone, et al. "An E2F7-Dependent Transcriptional Program Modulates DNA Damage Repair and Genomic Stability." *Nucleic Acids Research*, no. April, 2018, pp. 1–14, doi:10.1093/nar/gky218.

- Monvoisin, Arnaud, et al. "Involvement of Matrix Metalloproteinase Type-3 in Hepatocyte Growth Factor-Induced Invasion of Human Hepatocellular Carcinoma Cells." *International Journal of Cancer. Journal International Du Cancer*, vol. 97, no. 2, 2002, pp. 157–62, <http://www.ncbi.nlm.nih.gov/pubmed/11774258>.
- Moran, A., et al. "Risk of Cancer Other than Breast or Ovarian in Individuals with BRCA1 and BRCA2 Mutations." *Familial Cancer*, vol. 11, no. 2, 2012, pp. 235–42, doi:10.1007/s10689-011-9506-2.
- Mueller, Kristina M., Jan Wilhelm Kornfeld, et al. "Impairment of Hepatic Growth Hormone and Glucocorticoid Receptor Signaling Causes Steatosis and Hepatocellular Carcinoma in Mice." *Hepatology*, vol. 54, no. 4, 2011, pp. 1398–409, doi:10.1002/hep.24509.
- Mueller, Kristina M., Madeleine Themanns, et al. "Hepatic Growth Hormone and Glucocorticoid Receptor Signaling in Body Growth, Steatosis and Metabolic Liver Cancer Development." *Molecular and Cellular Endocrinology*, vol. 361, no. 1–2, 2012, pp. 1–11, doi:10.1016/j.mce.2012.03.026.
- Muz, Barbara, et al. "The Role of Hypoxia in Cancer Progression, Angiogenesis, Metastasis, and Resistance to Therapy." *Hypoxia*, 2015, p. 83, doi:10.2147/HP.S93413.
- Öhlund, Daniel, et al. "Fibroblast Heterogeneity in the Cancer Wound." *The Journal of Experimental Medicine*, vol. 211, no. 8, 2014, pp. 1503–23, doi:10.1084/jem.20140692.
- Okamoto, W., et al. "Differential Roles of STAT3 Depending on the Mechanism of STAT3 Activation in Gastric Cancer Cells." *British Journal of Cancer*, vol. 105, no. 3, 2011, pp. 407–12, doi:10.1038/bjc.2011.246.
- Orimo, Akira, et al. "Stromal Fibroblasts Present in Invasive Human Breast Carcinomas Promote Tumor Growth and Angiogenesis through Elevated SDF-1/CXCL12 Secretion." *Cell*, vol. 121, no. 3, 2005, pp. 335–48, doi:10.1016/j.cell.2005.02.034.
- Ozaki, I., et al. "Involvement of the Ets-1 Gene in Overexpression of Matrilysin in Human Hepatocellular Carcinoma." *Cancer Research*, vol. 60, no. 22, 2000, pp. 6519–25.
- Park, Catherine C., et al. "β1 integrin Inhibitory Antibody Induces Apoptosis of Breast Cancer Cells, Inhibits Growth, and Distinguishes Malignant from Normal Phenotype in Three Dimensional Cultures and in Vivo." *Cancer*

- Research, vol. 66, no. 3, 2006, pp. 1526–35, doi:10.1158/0008-5472.CAN-05-3071.
- Park, Hongryeol, et al. “Distinct Roles of DKK1 and DKK2 in Tumor Angiogenesis.” *Angiogenesis*, vol. 17, no. 1, 2014, pp. 221–34, doi:10.1007/s10456-013-9390-5.
- Paulus, W., et al. “Characterization of Integrin Receptors in Normal and Neoplastic Human Brain.” *Am J Pathol*, vol. 143, no. 1, 1993, pp. 154–63.
- Petrova, Varvara, et al. “The Hypoxic Tumour Microenvironment.” *Oncogenesis*, vol. 7, no. 1, 2018, doi:10.1038/s41389-017-0011-9.
- Phelan, C. M., et al. “Incidence of Colorectal Cancer in BRCA1 and BRCA2 Mutation Carriers: Results from a Follow-up Study.” *British Journal of Cancer*, vol. 110, no. 2, 2014, pp. 530–34, doi:10.1038/bjc.2013.741.
- Piret, J. P., et al. “CoCl<sub>2</sub>, a Chemical Inducer of Hypoxia-Inducible Factor-1, and Hypoxia Reduce Apoptotic Cell Death in Hepatoma Cell Line HepG2.” *Ann N Y Acad Sci*, vol. 973, 2002, pp. 443–47, doi:10.1111/j.1749-6632.2002.tb04680.x.
- Piret, Jean Pascal, et al. “Hypoxia and CoCl<sub>2</sub> protect HepG2 Cells against Serum Deprivation- and T-BHP-Induced Apoptosis: A Possible Anti-Apoptotic Role for HIF-1.” *Experimental Cell Research*, vol. 295, no. 2, 2004, pp. 340–49, doi:10.1016/j.yexcr.2004.01.024.
- Placencio, Veronica R., and Yves A. DeClerck. “Plasminogen Activator Inhibitor-1 in Cancer: Rationale and Insight for Future Therapeutic Testing.” *Cancer Research*, vol. 75, no. 15, 2015, pp. 2969–74, doi:10.1158/0008-5472.CAN-15-0876.
- Quail, D. F., and J. A. Joyce. “Microenvironmental Regulation of Tumor Progression and Metastasis.” *Nat Med*, vol. 19, no. 11, 2013, pp. 1423–37, doi:10.1038/nm.3394.
- Rajesh, Y., and Mahitosh Mandal. “Regulation of Extracellular Matrix Remodeling and Epithelial-Mesenchymal Transition by Matrix Metalloproteinases: Decisive Candidates in Tumor Progression.” *Proteases in Physiology and Pathology*, 2017, pp. 159–94, doi:10.1007/978-981-10-2513-6\_9.
- Rao, J. S. “Inhibition of Invasion, Angiogenesis, Tumor Growth, and Metastasis by Adenovirus-Mediated Transfer of Antisense uPAR and MMP-9 in Non-

- Small Cell Lung Cancer Cells.” *Molecular Cancer Therapeutics*, vol. 4, no. 9, 2005, pp. 1399–408, doi:10.1158/1535-7163.MCT-05-0082.
- Ravi, Maddaly, et al. “3D Cell Culture Systems: Advantages and Applications.” *Journal of Cellular Physiology*, vol. 230, no. 1, 2015, pp. 16–26, doi:10.1002/jcp.24683.
- Ridley, Anne J., et al. “Cell Migration: Integrating Signals from Front to Back.” *Science*, vol. 302, no. 5651, 2003, pp. 1704–09, doi:10.1126/science.1092053.
- Rondeau, S., et al. “ATM Has a Major Role in the Double-Strand Break Repair Pathway Dysregulation in Sporadic Breast Carcinomas and Is an Independent Prognostic Marker at Both mRNA and Protein Levels.” *British Journal of Cancer*, vol. 112, no. 6, 2015, pp. 1059–66, doi:10.1038/bjc.2015.60.
- Rudalska, Ramona, et al. “In Vivo RNAi Screening Identifies a Mechanism of Sorafenib Resistance in Liver Cancer.” *Nature Medicine*, vol. 20, no. 10, 2014, pp. 1138–46, doi:10.1038/nm.3679.
- Salnikow, Konstantin, et al. “Regulation of Hypoxia-Inducible Genes by ETS1 Transcription Factor.” *Carcinogenesis*, vol. 29, no. 8, 2008, pp. 1493–99, doi:10.1093/carcin/bgn088.
- Schaffner, Florence, et al. “Integrin  $\alpha 5 \beta 1$ , the Fibronectin Receptor, as a Pertinent Therapeutic Target in Solid Tumors.” *Cancers*, vol. 5, no. 1, 2013, pp. 27–47, doi:10.3390/cancers5010027.
- Schmidt-Arras, Dirk, and Stefan Rose-John. “IL-6 Pathway in the Liver: From Physiopathology to Therapy.” *Journal of Hepatology*, vol. 64, no. 6, 2016, pp. 1403–15, doi:10.1016/j.jhep.2016.02.004.
- Schmittgen, Thomas D., and Kenneth J. Livak. “Analyzing Real-Time PCR Data by the Comparative CT Method.” *Nature Protocols*, vol. 3, no. 6, 2008, pp. 1101–08, doi:10.1038/nprot.2008.73.
- Schwartz, Martin A., and Mark H. Ginsberg. “Networks and Crosstalk: Integrin Signalling Spreads.” *Nature Cell Biology*, vol. 4, no. 4, 2002, doi:10.1038/ncb0402-e65.
- Semenza, G. L. “Cancer-Stromal Cell Interactions Mediated by Hypoxia-Inducible Factors Promote Angiogenesis, Lymphangiogenesis, and Metastasis.” *Oncogene*, vol. 32, no. 35, 2013, pp. 4057–63, doi:10.1038/onc.2012.578.

- Shain, Kenneth H., et al. “ $\beta$ 1 Integrin Adhesion Enhances IL-6-Mediated STAT3 Signaling in Myeloma Cells: Implications for Microenvironment Influence on Tumor Survival and Proliferation.” *Cancer Research*, vol. 69, no. 3, 2009, pp. 1009–15, doi:10.1158/0008-5472.CAN-08-2419.
- Shi, Wen-Kai, et al. “PFKFB3 Blockade Inhibits Hepatocellular Carcinoma Growth by Impairing DNA Repair through AKT.” *Cell Death & Disease*, vol. 9, no. 4, Springer US, 2018, p. 428, doi:10.1038/s41419-018-0435-y.
- Shin, H. J., et al. “Carbonic Anhydrase IX (CA9) Modulates Tumor-Associated Cell Migration and Invasion.” *Journal of Cell Science*, vol. 124, no. 7, 2011, pp. 1077–87, doi:10.1242/jcs.072207.
- Song, Hoseok, et al. “p53 Gain-of-Function Cancer Mutants Induce Genetic Instability by Inactivating ATM.” *Nature Cell Biology*, vol. 9, no. 5, 2007, pp. 573–80, doi:10.1038/ncb1571.
- Span, Paul N., and Johan Bussink. “Biology of Hypoxia.” *Seminars in Nuclear Medicine*, vol. 45, no. 2, 2015, pp. 101–09, doi:10.1053/j.semnuclmed.2014.10.002.
- Stadler, Mira, et al. “Increased Complexity in Carcinomas: Analyzing and Modeling the Interaction of Human Cancer Cells with Their Microenvironment.” *Seminars in Cancer Biology*, vol. 35, 2015, pp. 107–24, doi:10.1016/j.semcancer.2015.08.007.
- Stepniak, Ewa, et al. “C-Jun/AP-1 Controls Liver Regeneration by Repressing p53/p21 and p38 MAPK Activity.” *Genes and Development*, vol. 20, no. 16, 2006, pp. 2306–14, doi:10.1101/gad.390506.
- Stiewe, Thorsten, et al. “Transactivation-Deficient DeltaTA-p73 Acts as an Oncogene.” *Cancer Research*, vol. 62, no. 13, 2002, pp. 3598–602.
- Thoma, Claudio R., et al. “3D Cell Culture Systems Modeling Tumor Growth Determinants in Cancer Target Discovery.” *Advanced Drug Delivery Reviews*, vol. 69–70, 2014, pp. 29–41, doi:10.1016/j.addr.2014.03.001.
- Thurlings, I., et al. “Synergistic Functions of E2F7 and E2F8 Are Critical to Suppress Stress-Induced Skin Cancer.” *Oncogene*, vol. 36, no. 6, 2017, pp. 829–39, doi:10.1038/onc.2016.251.
- Tomasini, Richard, et al. “TAp73 Knockout Shows Genomic Instability with Infertility and Tumor Suppressor Functions.” *Genes and Development*, vol. 22, no. 19, 2008, pp. 2677–91, doi:10.1101/gad.1695308.

- Tu, Kangsheng, et al. "Fibulin-5 Inhibits Hepatocellular Carcinoma Cell Migration and Invasion by down-Regulating Matrix Metalloproteinase-7 Expression." *BMC Cancer*, vol. 14, 2014, p. 938, doi:10.1186/1471-2407-14-938.
- Tu, Thomas, et al. "Novel Aspects of the Liver Microenvironment in Hepatocellular Carcinoma Pathogenesis and Development." *International Journal of Molecular Sciences*, vol. 15, no. 6, 2014, pp. 9422–58, doi:10.3390/ijms15069422.
- Tyndall, Joel, et al. "Peptides and Small Molecules Targeting the Plasminogen Activation System: Towards Prophylactic Anti-Metastasis Drugs for Breast Cancer." *Recent Patents on Anti-Cancer Drug Discovery*, vol. 3, no. 1, 2008, pp. 1–13, doi:10.2174/157489208783478711.
- Unger, Christine, et al. "Modeling Human Carcinomas: Physiologically Relevant 3D Models to Improve Anti-Cancer Drug Development." *Advanced Drug Delivery Reviews*, vol. 79, 2014, pp. 50–67, doi:10.1016/j.addr.2014.10.015.
- Vallo, Stefan, et al. "Blocking Integrin  $\beta$ 1 Decreases Adhesion in Chemoresistant Urothelial Cancer Cell Lines." *Oncology Letters*, vol. 14, no. 5, 2017, pp. 5513–18, doi:10.3892/ol.2017.6883.
- Vlahopoulos, Spiros A., et al. "The Role of ATF-2 in Oncogenesis." *BioEssays*, vol. 30, no. 4, 2008, pp. 314–27, doi:10.1002/bies.20734.
- Wang, L., et al. "Deficient DNA Damage Signaling Leads to Chemoresistance to Cisplatin in Oral Cancer." *Molecular Cancer Therapeutics*, vol. 11, no. 11, 2012, pp. 2401–09, doi:10.1158/1535-7163.MCT-12-0448.
- Wang, Maonan, et al. "Role of Tumor Microenvironment in Tumorigenesis." *Journal of Cancer*, vol. 8, no. 5, 2017, pp. 761–73, doi:10.7150/jca.17648.
- Weijts, Bart G. M. W., et al. "E2F7 and E2F8 Promote Angiogenesis through Transcriptional Activation of VEGFA in Cooperation with HIF1." *EMBO Journal*, vol. 31, no. 19, 2012, pp. 3871–84, doi:10.1038/emboj.2012.231.
- White, Donald E., et al. "Targeted Disruption of  $\beta$ 1-Integrin in a Transgenic Mouse Model of Human Breast Cancer Reveals an Essential Role in Mammary Tumor Induction." *Cancer Cell*, vol. 6, no. 2, 2004, pp. 159–70, doi:10.1016/j.ccr.2004.06.025.
- Wilson, Garrick K., et al. "Hypoxia Inducible Factors in Liver Disease and Hepatocellular Carcinoma: Current Understanding and Future Directions."



Journal of Hepatology, vol. 61, no. 6, 2014, pp. 1397–406, doi:10.1016/j.jhep.2014.08.025.

Wong, Carmen Chak Lui, et al. “The Impact of Hypoxia in Hepatocellular Carcinoma Metastasis.” *Frontiers of Medicine in China*, vol. 8, no. 1, 2014, pp. 33–41, doi:10.1007/s11684-013-0301-3.

Wykoff, Charles C., et al. “Hypoxia-Inducible Expression of Tumor-Associated Carbonic Anhydrases.” *Cancer Research*, vol. 60, no. 24, 2000, pp. 7075–83, doi:11156414.

Xia, Jianguo, et al. “NetworkAnalyst - Integrative Approaches for Protein-Protein Interaction Network Analysis and Visual Exploration.” *Nucleic Acids Research*, vol. 42, no. W1, 2014, doi:10.1093/nar/gku443.

Xu, Yingxi, et al. “STIM1 Accelerates Cell Senescence in a Remodeled Microenvironment but Enhances the Epithelial-to-Mesenchymal Transition in Prostate Cancer.” *Scientific Reports*, vol. 5, 2015, doi:10.1038/srep11754.

Yamaguchi, Kentaro, et al. “Histone Deacetylase Inhibitors Suppress the Induction of c-Jun and Its Target Genes Including COX-2.” *Journal of Biological Chemistry*, vol. 280, no. 38, 2005, pp. 32569–77, doi:10.1074/jbc.M503201200.

Yang, Annie, et al. “p63, a p53 Homolog at 3q27-29, Encodes Multiple Products with Transactivating, Death-Inducing, and Dominant-Negative Activities.” *Molecular Cell*, vol. 2, no. 3, 1998, pp. 305–16, doi:10.1016/S1097-2765(00)80275-0.

Yang, Changqing, et al. “Integrin  $\alpha 1\beta 1$  and  $\alpha 2\beta 1$  Are the Key Regulators of Hepatocarcinoma Cell Invasion Across the Fibrotic Matrix Microenvironment.” *Cancer Research*, vol. 63, no. 23, 2003, pp. 8312–17.

Yao, Jing, et al. “53BP1 Loss Induces Chemoresistance of Colorectal Cancer Cells to 5-Fluorouracil by Inhibiting the ATM–CHK2–P53 Pathway.” *Journal of Cancer Research and Clinical Oncology*, vol. 143, no. 3, 2017, pp. 419–31, doi:10.1007/s00432-016-2302-5.

Yeh, Chiu-an-ren, et al. “Fibroblast ER $\alpha$  Promotes Bladder Cancer Invasion via Increasing the CCL1 and IL-6 Signals in the Tumor Microenvironment.” *American Journal of Cancer Research*, vol. 5, no. 3, 2015, pp. 1146–57.

Zalmas, L., et al. “DNA-Damage Response Control of E2F7 and E2F8.” *EMBO Reports*, vol. 9, no. 3, 2008, pp. 252–59, doi:10.1038/sj.embor.7401158.

- Zhang, Jing, and Jinsong Liu. "Tumor Stroma as Targets for Cancer Therapy." *Pharmacology & Therapeutics*, vol. 137, no. 2, 2013, pp. 200–15, doi:10.1016/j.pharmthera.2012.10.003.
- Zhang, Qi, et al. "Wnt/ $\beta$ -Catenin Signaling Enhances Hypoxia-Induced Epithelial-Mesenchymal Transition in Hepatocellular Carcinoma via Crosstalk with Hif-1 $\alpha$  Signaling." *Carcinogenesis*, vol. 34, no. 5, 2013, pp. 962–73, doi:10.1093/carcin/bgt027.
- Zheng, L., et al. "miRNA-145 Targets v-Ets Erythroblastosis Virus E26 Oncogene Homolog 1 to Suppress the Invasion, Metastasis, and Angiogenesis of Gastric Cancer Cells." *Molecular Cancer Research*, vol. 11, no. 2, 2013, pp. 182–93, doi:10.1158/1541-7786.MCR-12-0534.
- Zheng, Q., et al. "Invasion and Metastasis of Hepatocellular Carcinoma in Relation to Urokinase-Type Plasminogen Activator, Its Receptor and Inhibitor." *Journal of Cancer Research and Clinical Oncology*, vol. 126, no. 11, 2000, pp. 641–46.